Bioconjugate Chemistry

Article

pubs.acs.org/bc

Paradoxical Downregulation of CXC Chemokine Receptor 4 Induced by Polyphemusin II-Derived Antagonists

Ryo Masuda,[†] Shinya Oishi,*[,†] Noriko Tanahara,[†] Hiroaki Ohno,[†] Akira Hirasawa,[†] Gozoh Tsujimoto,[†] Yoshiaki Yano,[†] Katsumi Matsuzaki,[†] Jean-Marc Navenot,[‡] Stephen C. Peiper,[‡] and Nobutaka Fujii*[,†]

[†]Graduate School of Pharmaceutical Sciences, Kyoto University, Sakyo-ku, Kyoto 606-8501, Japan

[‡]Department of Pathology, Anatomy and Cell Biology, Thomas Jefferson University, Philadelphia, Pennsylvania 19107, United States

Supporting Information

ABSTRACT: CXC chemokine receptor 4 (CXCR4) is a G protein-coupled receptor implicated in cell entry of T-cell line-tropic HIV-1 strains. CXCR4 and its ligand stromal cell derived factor-1 (SDF-1)/CXCL12 play pivotal parts in many physiological processes and pathogenetic conditions (e.g., immune cell-homing and cancer metastasis). We previously developed the potent CXCR4 antagonist T140 from structure–activity relationship studies of the antimicrobial peptide polyphemusin II. T140 and its derivatives have been exploited in biological and biomedical studies for the SDF-1/CXCR4 axis. We investigated receptor localization upon ligand stimulation using fluorescent SDF-1 and T140 derivatives as well as a specific labeling technique for cellular-membrane CXCR4. Fluorescent T140 derivatives induced translocation of CXCR4 into the perinuclear region as observed by treatment with fluorescent SDF-1. T140 derivative-mediated internalization of CXCR4 was also monitored by the coiled-coil tag-probe system. These findings demonstrated that the CXCR4 antagonistic activity and anti-HIV activity of T140 derivatives were derived (at least in part) from antagonist-mediated receptor internalization.

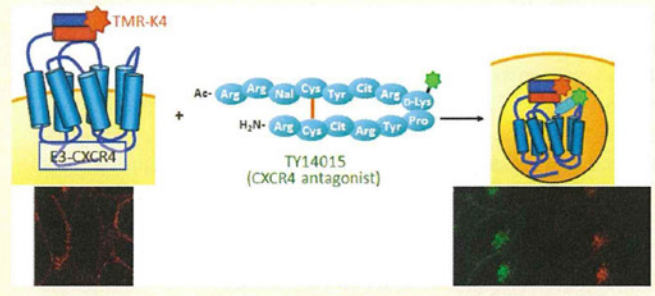

INTRODUCTION

CXC chemokine receptor 4 (CXCR4) is a G-protein-coupled receptor. It is widely expressed in leukocytes such as T-cells, B-cells, and monocytes.[1,2] Under physiological conditions, the endogenous ligand, stromal cell-derived factor-1 (SDF-1)/CXCL12, is secreted by bone marrow stromal cells for expansion and development of precursor B-cells.[3] High concentrations of SDF-1 are present at inflammatory sites, so the migration of CXCR4-expressing stem cells toward an SDF-1 gradient promotes repair of injured tissues.[4] There have been many reports on the pathology of CXCR4-related cancer, including CXCR4 overexpression and organ-specific metastasis among various types of cancer cells.[5,6] During metastasis, SDF-1 from secondary lesions functions as a chemoattractant for directional migration of CXCR4-expressing malignant cells.[5,6]

The activation process of CXCR4 by SDF-1 has been well documented.[7] Upon SDF-1 binding, CXCR4 evokes downstream signaling via dissociation of heterotrimeric G proteins, followed by decrease in intracellular cyclic adenosine monophosphate (cAMP) concentrations, upregulation of Ca^{2+} release, and increase in extracellular-signal-regulated kinase (ERK) 1/2 phosphorylations.[8−10] Furthermore, CXCR4 internalization in response to SDF-1 occurs in early endosomes through β-arrestin recruitment, just like other GPCRs,[11] in which phosphorylated serine residues and a dileucine motif at the CXCR4 C-terminus have critical roles.[12,13] The complex is sorted into late endosomes/lysosomes for the degradation pathway or for recycling endosomes.[11,14] In addition, CXCR4 is used as a major co-receptor for the entry of T-cell line tropic human immunodeficiency virus type 1 (HIV-1) into target host cells.[15,16] The inhibitory effect of SDF-1 on HIV infection is thought to be by competitive binding to CXCR4 as well as CXCR4 downregulation.[17,18] CXCR4 is a promising molecular target for potential anti-metastatic agents and anti-HIV agents, so several CXCR4 ligands have been developed.[5,19−22]

We previously developed the potent anti-HIV peptide T140. This was designed from the structure–activity relationship studies of a self-defense peptide of horseshoe crabs, polyphemusin II (Figure 1).[19] Inhibition of HIV-induced cytopathogenicity by T140 and its derivatives was derived from selective CXCR4 antagonistic and/or inverse agonistic activity (in which the basal signal levels were decreased in the guanosine triphosphate (GTP) binding and intracellular calcium flux assay using a constitutively active mutant).[23] A recent report on the crystal structure of CXCR4 in complex with the T140 derivative CVX15 revealed that arginine residues in CVX15 made polar interactions with Asp171 and Asp187 in CXCR4.[24] Point-mutation experiments of CXCR4 revealed that additional residues on the extracellular domain (Arg188, Gly207, and Asp262) are necessary for the interaction of

Received: February 18, 2012
Revised: April 7, 2012
Published: April 10, 2012

H-Arg-Arg-Nal-Cys-Tyr-Arg-Lys-D-Lys-Pro-Tyr-Arg-Cit-Cys-Arg-OH T140
H-Arg-Arg-Nal-Cys-Tyr-Gln-Lys-D-Pro-Pro-Tyr-Arg-Cit-Cys-Arg-Gly-D-Pro-OH CVX15
4FBz-Arg-Arg-Nal-Cys-Tyr-Cit-Lys-D-Lys-Pro-Tyr-Arg-Cit-Cys-Arg-NH_2 TF14016
R
Ac-Arg-Arg-Nal-Cys-Tyr-Cit-Arg-D-Lys-Pro-Tyr-Arg-Cit-Cys-Arg-NH_2 TY14015 (R = AF488)
TR14011 (R = TMR)

Figure 1. Amino acid sequences of CXCR4 antagonist peptides. The disulfide bonds between cysteine residues are shown by solid lines. D-Amino acids are not first-letter capitalized. Abbreviations: Nal, L-3-(2-naphthyl)alanine; Cit, L-citrulline; 4FBz, 4-fluorobenzoyl; AF488, AlexaFluor 488; TMR, tetramethylrhodamine.

T140, which is independent of the interaction with SDF-1.[25,26] These residues contribute to stabilization of the CXCR4 structure via formation of hydrogen bonds with adjacent residues, so T140 binding to these residues may impair SDF-1 binding via conformational changes of CXCR4. ALX-40C is an alternative CXCR4 antagonist that inhibits HIV-1 infection into T-cells.[27] The anti-HIV activity of ALX-40C with a sequence of nine D-Arg is also reported to be derived from binding to acidic residues in the second extracellular loop of CXCR4.[27]

It was demonstrated that highly basic peptides such as ALX-40C and HIV-1 Tat translocate into the intracellular compartment through endocytosis.[28−31] On the basis of the biological properties of these highly basic peptides, we assumed that polyphemusin II-derived CXCR4 antagonists could induce the internalization and/or translocation of receptors into the intracellular compartment, resulting in the apparent antagonistic or inverse agonistic activity for CXCR4.

In the present study, we investigated the mechanism of action of T140 derivatives using novel fluorescent probes. The uptake and localization of CXCR4 was monitored by analyses of flow cytometry and confocal microscopy using the coiled-coil tag-probe system[32] for the labeling of cell-surface CXCR4.

EXPERIMENTAL SECTION

Quantitative Analyses of Cell-Surface E3-CXCR4 Using a Fluorescent K4-Peptide by Flow Cytometry. E3-CXCR4 CHO cells were detached using versene and incubated with 100 nM FL-K4 in F-12 medium (500 μL) at 0 °C for 15 min in the absence or presence of unlabeled K4-peptide or SDF-1. The intensity of cell staining was analyzed using a FACScalibur system (BD Biosciences, San Jose, CA, USA). Ten thousand events per sample were analyzed, and the data collected from FL1 in log mode. Fluorescent intensity was calculated as a geometric mean of cellular fluorescence. Data were analyzed using *CellQuest Pro* software (BD Biosciences). Data were analyzed using a two-tailed Student's *t* test with significance set at $p \leq 0.05$.

Quantitative Analyses of Ligand-Mediated CXCR4 Internalization by Flow Cytometry. E3-CXCR4 CHO cells were detached using versene and resuspended in F-12 medium (100 μL) containing each ligand. After incubation at 37 °C for 30 min, ice-cold F-12 medium (400 μL) was added to the mixture, and cells centrifuged at 500 × *g* for 5 min at 4 °C. Cell pellets were then incubated with 100 nM FL-K4 in F-12 (100 μL) at 0 °C for 15 min. The mixture was diluted with ice-cold F-12 medium (400 μL), and analyzed using a FACScalibur flow cytometer.

Binding and Displacement of [^{125}I]-SDF-1. A membrane fraction of cells expressing CXCR4 was incubated with 0.5 nM of [^{125}I]-SDF-1 and FL-K4 in binding buffer [50 mM HEPES (pH 7.4), 5 mM $MgCl_2$, 1 mM $CaCl_2$, and 0.1% bovine serum albumin (BSA) in H_2O] for 1 h at room temperature. Reaction mixtures were filtered through GF/B filters (PerkinElmer, Waltham, MA, USA) pretreated with 0.1% polyethyleneimine. The filter plate was washed with wash buffer [50 mM HEPES (pH 7.4), 500 mM NaCl, and 0.1% BSA in H_2O] and bound radioactivity measured by TopCount (PerkinElmer).

Confocal Microscopy Analyses of Ligand and CXCR4 Internalization. E3-CXCR4 CHO cells were plated on 35 mm glass-bottomed dishes and cultured in F-12 medium containing 10% heat-inactivated fetal bovine serum supplemented with penicillin/streptomycin and hygromycin. Cells were washed once with cold F-12 medium, and incubated with fluorescent ligands [SDF-1^{AF488} (100 nM) or TY14015 (1 μM)] in F-12 medium (100 μL) at 30 °C for 30 min. After rinsing once with cold F-12 medium, cells were observed by confocal microscopy (Eclipse Ti-E: Nikon, Tokyo, Japan). To monitor CXCR4 localization, E3-CXCR4 CHO cells were pretreated with 100 nM fluorescent K4-peptide in F-12 medium (100 μL) at 0 °C for 15 min before treatment with CXCR4 ligands.

For staining of cellular compartments, after incubation with fluorescent ligands or K4-peptide, cells were rinsed once with cold F-12 medium and treated with the marker (FM 4−64 for the cell membrane; LysoTracker Red DND-99 for lysosomes; ER-tracker Red for the endoplasmic reticulum; or AlexaFluor 568-conjugated transferrin for endosomes) according to the manufacturer (Invitrogen, Carlsbad, CA, USA, for all markers) protocol. The green (AlexaFluor 488 and ATTO488) channel was excited by a 488 nm laser and detected through a BP 500−550 nm emission filter. The red (TMR and AlexaFluor 568) channel was excited by a 568 nm laser, and detected through a BP 575−605 nm emission filter. The blue (FM 4−64) channel was excited by a 568 nm laser, and detected through a LP 665 nm emission filter. Data were analyzed using *EZ-C1 Viewer* software (Nikon).

RESULTS

Labeling of Cell-Membrane CXCR4 by the Coiled-Coil Tag-Probe System. A stable CXCR4-expressing cell line was established to monitor the internalization of CXCR4. The surface-exposed tag sequence E3 $(EIAALEK)_3$ was appended at the N-terminus of CXCR4 for detection using the peptide probe K4 $(KIAALKE)_4$ with an appropriate tracer group.[32] This coiled-coil tag-probe system provides several distinct advantages to visualize cell-surface CXCR4. For example, K4-peptide is much smaller than anti-epitope antibodies, so ligand binding to the receptor is hardly disturbed. In addition, specific labeling of E3-tagged receptors on cell membranes with fluorescent K4-peptides can distinguish the internalized receptor from the receptor that is originally present in the cytosolic compartment. This is in contrast to receptors fused with fluorescent proteins, which have usually been employed for monitoring receptor localization.[14,33]

CHO cells stably expressing E3-tagged CXCR4 (E3-CXCR4) were generated by the Flp-In expression system, and were studied by flow cytometric analyses. E3-CXCR4

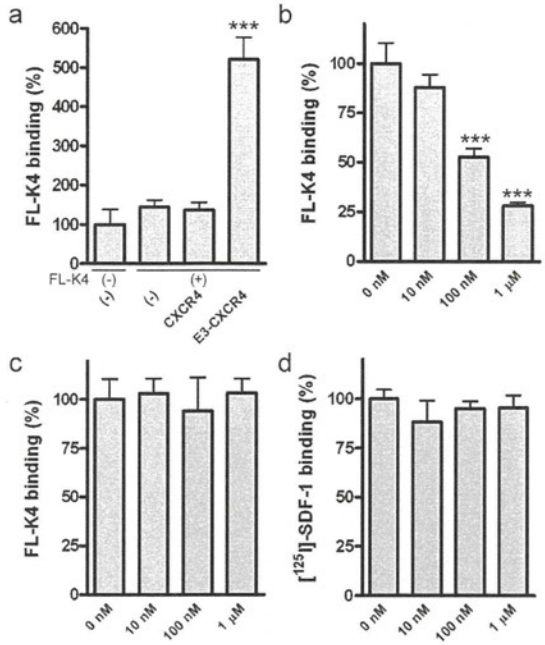

Figure 2. Labeling of E3-CXCR4 cells with fluorescein-K4-peptide (FL-K4). (a) FL-K4 binding to CXCR4 cell lines. After cells were treated with FL-K4 (100 nM) at 0 °C for 15 min, bound FL-K4 was measured by flow cytometry. (b) Inhibition of FL-K4 binding to E3-CXCR4 by unlabeled K4-peptide. After E3-CXCR4 CHO cells were labeled with FL-K4 (100 nM) in the presence of various concentrations of unlabeled K4-peptide at 0 °C for 15 min, bound FL-K4 was measured by flow cytometry. (c) Effect of SDF-1 on FL-K4 binding to E3-CXCR4. After E3-CXCR4 CHO cells were labeled with FL-K4 (100 nM) in the presence of various concentrations of SDF-1 at 0 °C for 15 min, bound various concentrations of FL-K4 was measured by flow cytometry. (d) Effect of K4-peptide on SDF-1 binding to E3-CXCR4. [^{125}I]-SDF-1 (0.5 nM) binding to E3-CXCR4. (±S.D., n = 3; *** $p \leq 0.005$).

CHO cells were clearly seen to be stained by fluorescein-conjugated K4-peptide (FL-K4) (Figure 2a). This staining was inhibited by unlabeled K4-peptide in a dose-dependent manner, suggesting specific labeling of E3-CXCR4 by interaction between E3-tag and K4-peptide (Figure 2b). FL-K4 binding to E3-CXCR4 was not disturbed by SDF-1 even at 1 μM, which demonstrated that FL-K4-mediated staining was independent of SDF-1 binding to CXCR4 (Figure 2c). SDF-1 binding to E3-CXCR4 was also unaffected by K4-peptide, which was verified by the binding inhibition assay using [^{125}I]-SDF-1 (Figure 2d). Taken together, specific fluorescent labeling of CXCR4 was accomplished by the coiled-coil tag-probe system without mutual competitive inhibition of SDF-1 and K4-peptide binding to the receptor.

Monitoring and Quantitative Analyses of SDF-1-Induced CXCR4 Internalization. The level of residual CXCR4 on the cell membrane after SDF-1 stimulation has been measured by flow cytometry using a CXCR4-specific antibody.[34,35] For example, Honczarenko et al. assessed SDF-1-induced internalization of CXCR4 by staining cell-surface CXCR4 by the monoclonal antibody 12G5.[34] However, the possible competitive binding of SDF-1 and antibody to cell-surface CXCR4 may impair receptor detection. To overcome this potential disadvantage, the coiled-coil tag-probe pair system could be an alternative to quantify cell-surface CXCR4.

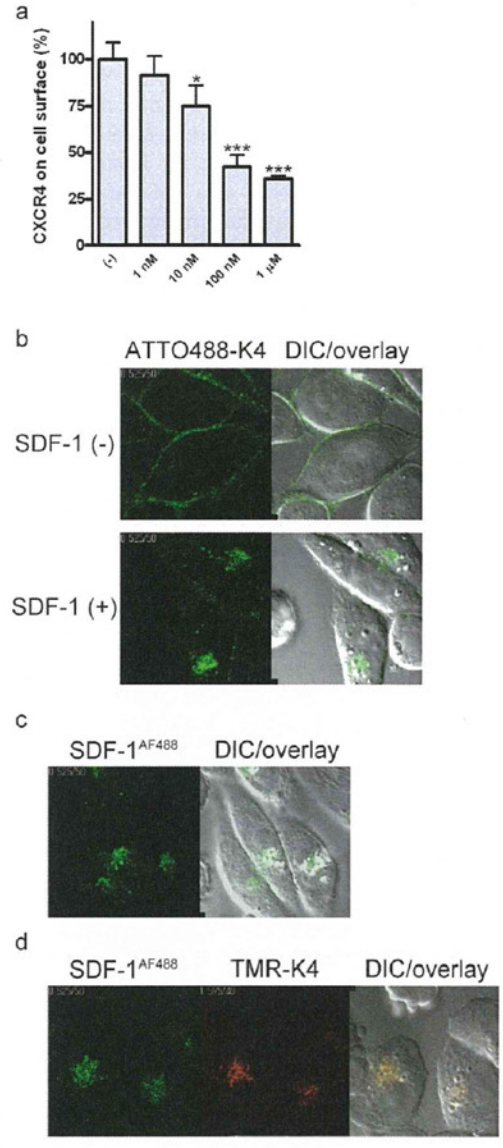

Figure 3. CXCR4 internalization induced by SDF-1 derivatives. (a) Quantitative analyses of E3-CXCR4 internalization by flow cytometry. After E3-CXCR4 CHO cells were treated with various concentrations of SDF-1 at 37 °C for 30 min, cells were labeled by FL-K4 (100 nM) at 0 °C for 15 min (±S.D., n = 3; * $p \leq 0.05$; *** $p \leq 0.005$). (b) Confocal microscopy images of SDF-1-mediated CXCR4 internalization. After E3-CXCR4-expressing cells were labeled with ATTO488-K4 (100 nM) at 0 °C for 15 min, cells were treated with SDF-1 (100 nM) at 30 °C for 30 min. (c) Confocal microscopy images of internalized fluorescent SDF-1. E3-CXCR4-expressing cells were treated with SDF-1^{AF488} (100 nM) for 30 min. (d) Confocal microscopy images of internalized SDF-1 (green) and CXCR4 (red). After E3-CXCR4-expressing cells were labeled with TMR-K4 (100 nM) at 0 °C for 15 min, and cells were treated with SDF-1^{AF488} (100 nM) at 30 °C for 30 min. Representative z-slice confocal microscopy images are shown.

SDF-1-mediated CXCR4 internalization was investigated using the established system. Initially, quantitative analyses of residual cell-surface E3-CXCR4 after SDF-1 stimulation were undertaken by flow cytometry. Cells were stained with FL-K4 after E3-CXCR4 CHO cells were treated with SDF-1 over a range of concentrations. The fluorescent intensity of FL-K4 was significantly decreased in a dose-dependent manner (Figure 3a). Confocal microscopy studies using ATTO488-conjugated

K4-peptide (ATTO488-K4) confirmed the translocation of E3-CXCR4 to the intracellular compartment by treatment with SDF-1, whereas ATTO488-K4/E3-CXCR4 remained on the cell surface without SDF-1 treatment (Figure 3b). Both results suggested that SDF-1 stimulation induced FL-K4 labeled E3-CXCR4 internalization, and that the E3 sequence on the N-terminus of CXCR4 could work as a functional tag to detect receptor localization without disturbing receptor internalization.

CXCR4 internalization was also monitored by confocal microscopy using a fluorescent SDF-1 derivative.[36] Translocation of SDF-1^{AF488} into the intracellular compartment was observed by treatment of E3-CXCR4 cells (without labeling by fluorescent K4-peptide) (Figure 3c). This was consistent with the SDF-1-mediated internalization of FL-K4-labeled E3-CXCR4 (Figure 3b). The intracellular localization of SDF-1^{AF488} was not observed in CHO cells without CXCR4 expression (see Supporting Information, Supplementary Figure 1). Hence, it could be concluded that this translocation was mediated by the interaction with CXCR4. To confirm the colocalization of SDF-1 and CXCR4, the same experiment was conducted using E3-CXCR4-expressing cells labeled with TMR-conjugated K4-peptide (TMR-K4). Incubation of cells with SDF-1^{AF488} induced translocation of TMR-K4/E3-CXCR4 complexes into the intracellular compartment, which was verified by colocalization of SDF-1^{AF488} and TMR-K4/E3-CXCR4 (Figure 3d). An identical phenotype was observed in an experiment using SDF-1^{TMR} and ATTO488-K4/E3-CXCR4, indicating that the fluorophore functional groups on the ligand and receptor did not influence the translocation (see Supporting Information, Supplementary Figure 2).

Polyphemusin-Derived CXCR4 Antagonists Induce Receptor Internalization. Next, we investigated receptor internalization by CXCR4 antagonists using the coiled-coil tag-probe system. E3-CXCR4 CHO cells were treated with polyphemusin II and CXCR4 antagonists (TF14016[37] or FC131[38]) at 37 °C. The proportion of residual receptors on the cell membrane was subsequently determined by flow cytometry in the presence of FL-K4 (Figure 4a). The fluorescence intensity of FL-K4 was reduced by 20−25% by the antagonists.[39] In contrast, a decrease in FL-K4 fluorescence was not observed in the same experiment at 0 °C, in which receptor internalization does not occur,[40] suggesting that the E3-tag/K4-peptide interaction was not inhibited by the antagonists. Antagonist-induced internalization was also confirmed by fluorescence microscopy analyses of ATTO488-K4/E3-CXCR4 CHO cells. TF14016 induced the translocation of ATTO488-K4/E3-CXCR4 into the perinuclear region, just like that seen in SDF-1 stimulation (Figure 4b). As such, it was demonstrated that CXCR4 antagonists partially induced receptor internalization.

The fluorescent CXCR4 antagonist TY14015 was similarly accumulated in the cytosolic perinuclear domain in E3-CXCR4 CHO cells after 30 min incubation at 30 °C (Figure 4c). TY14015-mediated translocation was not observed in the same experiments using nontransfected CHO cells,[41] nor by incubation of E3-CXCR4 CHO cells with TY14015 at 0 °C (see Supporting Information, Supplementary Figure 1). These findings indicated that CXCR4 serves as an essential receptor for the translocation of CXCR4 antagonists by an active pathway such as endocytosis. In contrast to the experiment using SDF-1^{AF488} (Figure 3c), staining of the cell membrane by TY14015 was also observed (Figure 4c).

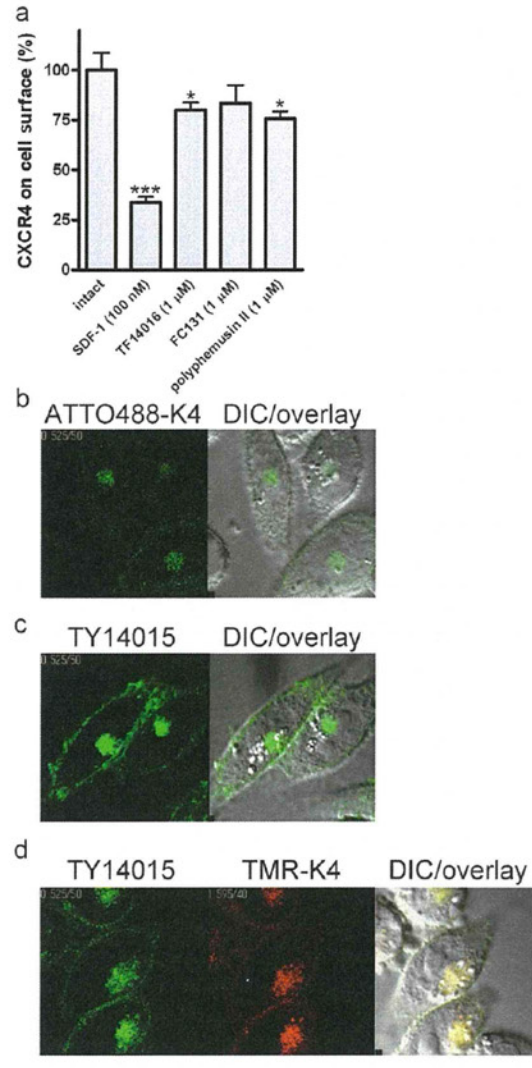

Figure 4. CXCR4 internalization upon stimulation by CXCR4 antagonists. (a) Quantitative analyses of E3-CXCR4 internalization by flow cytometry. After E3-CXCR4 CHO cells were treated with each antagonist (1 μM) at 37 °C for 30 min, and cells were labeled by FL-K4 (100 nM) at 0 °C for 15 min (±S.D., $n = 3$; * $p \leq 0.05$; *** $p \leq 0.005$). (b) Confocal microscopy images of TF14016-mediated CXCR4 internalization. After E3-CXCR4 CHO cells were labeled with ATTO488-K4 (100 nM) at 0 °C for 15 min, cells were treated with TF14016 (1 μM) at 30 °C for 30 min. (c) Confocal microscopy images of internalized TY14015. E3-CXCR4 CHO cells were treated with TY14015 (1 μM) at 30 °C for 30 min. (d) Confocal microscopy images of internalized TY14015 (green) and CXCR4 (red). After E3-CXCR4 CHO cells were labeled with TMR-K4 (100 nM) at 0 °C for 15 min, cells were treated with TY14015 (1 μM) at 30 °C for 30 min. Representative z-slice confocal microscopy images are shown.

The localization of fluorescent T140 derivatives and CXCR4 was simultaneously monitored by confocal microscopy using the coiled-coil tag-probe system. After preincubation with TMR-K4, E3-CXCR4 CHO cells were stimulated by TY14015. Merged confocal microscopy images revealed that TY14015 colocalized with TMR-K4/E3-CXCR4 (Figure 4d). This colocalization was not affected by the fluorophores, which was verified by experiments using ATTO488-K4/E3-CXCR4 and TR14011 (Figure 1, see also Supporting Information, Supplementary Figure 2). CXCR4-Venus CHO cells (in which a fluorescent Venus protein was fused at the C-terminus of CXCR4) showed an identical phenotype upon stimulation with

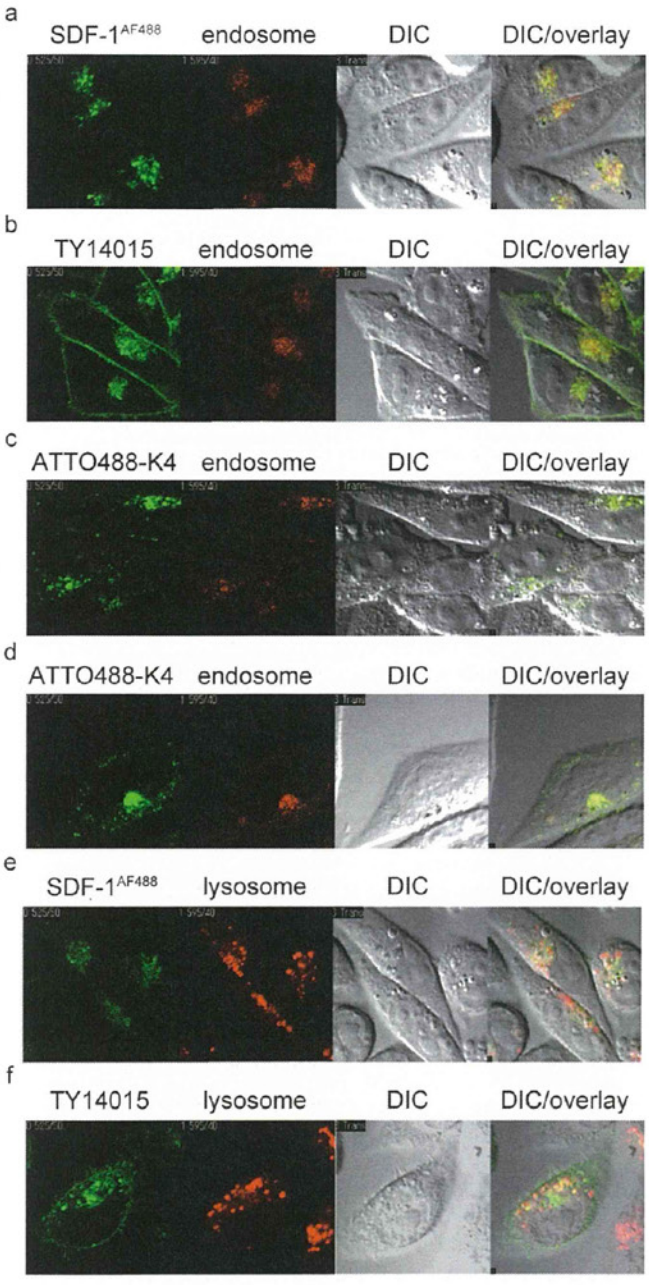

Figure 5. Translocation of fluorescent CXCR4 ligands and the receptor. (a,b) Confocal microscopy images of SDF-1^{AF488} (a) or TY14015 (b) and endosome. After E3-CXCR4 CHO cells were treated with fluorescent ligands at 30 °C for 30 min, cells were stained with AlexaFluor 568-transferrin (50 μg/mL) for 60 min. (c,d) Confocal microscopy images of internalized CXCR4 and endosome after stimulation with SDF-1 (c) or TF14016 (d). After E3-CXCR4 CHO cells were labeled with ATTO488-K4 (100 nM) at 0 °C for 15 min, cells were treated with ligand at 30 °C for 30 min and stained with AlexaFluor 568-transferrin (50 μg/mL) for 60 min. (e,f) Confocal microscopy images of SDF-1^{AF488} (e) or TY14015 (f) and lysosome. After E3-CXCR4 CHO cells were treated with fluorescent ligands at 30 °C for 30 min, cells were stained with LysoTracker (1 μM) for 30 min. Representative *z*-slice confocal microscopy images are shown.

SDF-1^{TMR} or TR14011 (see Supporting Information, Supplementary Figure 2). These data suggested that T140 derivatives translocated into the intracellular compartment with formation of ligand–receptor complexes.

Intracellular Translocation of CXCR4 Ligands and Receptor. The intracellular destination of CXCR4 ligand–receptor complexes after the binding of CXCR4 antagonists was investigated by confocal microscopy (Figure 5; see also Supporting Information, Supplementary Figure 3). After E3-CXCR4 CHO cells were treated with CXCR4 ligands, cells were stained with several organelle-specific fluorescent markers. SDF-1^{AF488} translocated to endosomal compartments in 30 min, which were stained by AlexaFluor 568-conjugated transferrin (Figure 5a). This result was in agreement with another report on SDF-1-mediated CXCR4 internalization.[17] Similarly, TY14015 accumulated in the same intracellular compartment (Figure 5b). Localization of ATTO-K4/E3-CXCR4 after treatment with SDF-1 and TF14016 was also similar to the distribution of transferrin, indicating that internalized CXCR4 ligand–receptor complexes translocate into endosomal compartments (Figure 5c,d). Meanwhile, localization of the fluorescent CXCR4 ligands in lysosomes was partial (Figure 5e,f). Agonists and antagonists of CXCR4 may indirectly affect the distributions of lysosomes. Staining with FM 4–64 or ER-trackers suggested that SDF-1^{AF488} existed neither on the cell membrane nor in the endoplasmic reticulum, whereas partial staining with TY14015 on cell membranes was observed (see Supporting Information, Supplementary Figure 3).

■ DISCUSSION

Agonist-mediated internalization of GPCRs induces the transduction of downstream signaling and desensitization to regulate cell homeostasis. In contrast, reports on antagonist-induced receptor internalization (e.g., cholecystokinin A, 5-HT_{2A}, and neuropeptide Y_1 receptors) are limited.[42−44] This is the first report on the antagonist-mediated internalization of CXCR4. A series of polyphemusin II-derived and other CXCR4 antagonists contain basic functional groups such as arginine and lysine residues, which are involved in the interactions with the extracellular domain of CXCR4-bearing negative charges. In the present study, using the coiled-coil tag-probe system to visualize cell-surface CXCR4, CXCR4-mediated translocation of T140 derivatives into intracellular compartments was demonstrated. Although the internalization effect of surface CXCR4 by T140 derivatives was partial (only 25%, much less than the agonist SDF-1), this CXCR4 internalization supports the apparent antagonistic activity of T140 derivatives against SDF-1 binding to CXCR4 as well as the induction of inverse agonistic activity signaling.[23] It was reported that treatment of CXCR4-expressing cells with HIV-1 gp120 peptide induces similar CXCR4 internalization without agonistic activity, which is closely related to HIV infection.[14] Although T140 derivatives have been thought to be competitive inhibitors against gp120 binding to CXCR4,[19] antagonist-mediated internalization of cell-surface CXCR4 could be an alternative mode of action for anti-HIV activity.[17,18] Further investigation of the mechanisms of this paradoxical antagonist-mediated down-regulation of CXCR4 could facilitate development of novel anti-metastatic and anti-HIV agents.

■ ASSOCIATED CONTENT

Ⓢ Supporting Information

Experimental procedures as well as confocal microscopy images of ligand and receptor internalization in the control experiments. This material is available free of charge via the Internet at http://pubs.acs.org.

AUTHOR INFORMATION

Corresponding Author

*Tel: +81-75-753-4551, Fax: +81-75-753-4570, E-mail: soishi@pharm.kyoto-u.ac.jp (S.O.), nfujii@pharm.kyoto-u.ac.jp (N.F.).

Notes

The authors declare no competing financial interest.

ACKNOWLEDGMENTS

We thank Prof. Shiroh Futaki and Dr. Ikuhiko Nakase (Institute for Chemical Research, Kyoto University) for excellent technical advices. This work was supported by Grants-in-Aid for Scientific Research and Targeted Proteins Research Program from the Ministry of Education, Culture, Sports, Science, and Technology of Japan; and by a grant for Promotion of AIDS Research from the Ministry of Health and Welfare of Japan. R.M. is grateful for Research Fellowships from the JSPS for Young Scientists.

REFERENCES

(1) Viola, A., and Luster, A. D. (2008) Chemokines and their receptors: drug targets in immunity and inflammation. *Annu. Rev. Pharmacol. Toxicol. 48*, 171−197.

(2) Bleul, C. C., Farzan, M., Choe, H., Parolin, C., Clark-Lewis, I., Sodroski, J., and Springer, T. A. (1996) The lymphocyte chemoattractant SDF-1 is a ligand for LESTR/fusin and blocks HIV-1 entry. *Nature 382*, 829−833.

(3) Egawa, T., Kawabata, K., Kawamoto, H., Amada, K., Okamoto, R., Fujii, N., Kishimoto, T., Katsura, Y., and Nagasawa, T. (2001) The earliest stages of B cell development require a chemokine stromal cell-derived factor/pre-B cell growth-stimulating factor. *Immunity 15*, 323−334.

(4) Ratajczak, M. Z., Majka, M., Kucia, M., Drukala, J., Pietrzkowski, Z., Peiper, S., and Janowska-Wieczorek, A. (2003) Expression of functional CXCR4 by muscle satellite cells and secretion of SDF-1 by muscle-derived fibroblasts is associated with the presence of both muscle progenitors in bone marrow and hematopoietic stem/progenitor cells in muscles. *Stem Cells 21*, 363−371.

(5) Rubin, J. B., Kung, A. L., Klein, R. S., Chan, J. A., Sun, Y., Schmidt, K., Kieran, M. W., Luster, A. D., and Segal, R. A. (2003) A small-molecule antagonist of CXCR4 inhibits intracranial growth of primary brain tumors. *Proc. Natl. Acad. Sci. U. S. A. 100*, 13513−13518.

(6) Monaco, G., Belmont, J. W., Konopleva, M., Andreeff, M., Tavor, S., Petit, I., Kollet, O., and Lapidot, T. (2004) Correlation between CXCR4 and homing or engraftment of acute myelogenous leukemia. *Cancer Res. 64*, 6832−6833.

(7) Busillo, J. M., and Benovic, J. L. (2007) Regulation of CXCR4 signaling. *Biochim. Biophys. Acta 1768*, 952−963.

(8) Rollins, B. J. (1997) Chemokines. *Blood 90*, 909−928.

(9) Dwinell, M. B., Ogawa, H., Barrett, K. E., and Kagnoff, M. F. (2004) SDF-1/CXCL12 regulates cAMP production and ion transport in intestinal epithelial cells via CXCR4. *Am. J. Physiol. Gastrointest. Liver Physiol. 286*, 844−850.

(10) Busillo, J. M., Armando, S., Sengupta, R., Meucci, O., Bouvier, M., and Benovic, J. L. (2010) Site-specific phosphorylation of CXCR4 is dynamically regulated by multiple kinases and results in differential modulation of CXCR4 signaling. *J. Biol. Chem. 285*, 7805−7817.

(11) Kumar, A., Kremer, K. N., Dominguez, D., Tadi, M., and Hedin, K. E. (2011) Gα13 and Rho mediate endosomal trafficking of CXCR4 into Rab11+ vesicles upon stromal cell-derived factor-1 stimulation. *J. Immunol. 186*, 951−958.

(12) Marchese, A., and Benovic, J. L. (2001) Agonist-promoted ubiquitination of the G protein-coupled receptor CXCR4 mediates lysosomal sorting. *J. Biol. Chem. 276*, 45509−45512.

(13) Orsini, M. J., Parent, J. L., Mundell, S. J., Marchese, A., and Benovic, J. L. (1999) Trafficking of the HIV coreceptor CXCR4. Role of arrestins and identification of residues in the C-terminal tail that mediate receptor internalization. *J. Biol. Chem. 274*, 31076−31086.

(14) Tarasova, N. I., Stauber, R. H., and Michejda, C. J. (1998) Spontaneous and ligand-induced trafficking of CXC-chemokine receptor 4. *J. Biol. Chem. 273*, 15883−15886.

(15) Feng, Y., Broder, C. C., Kennedy, P. E., and Berger, E. A. (1996) HIV-1 entry cofactor: functional cDNA cloning of a seven-transmembrane, G protein-coupled receptor. *Science 272*, 872−877.

(16) Berson, J. F., Long, D., Doranz, B. J., Rucker, J., Jirik, F. R., and Doms, R. W. (1996) A seven-transmembrane domain receptor involved in fusion and entry of T-cell-tropic human immunodeficiency virus type 1 strains. *J. Virol. 70*, 6288−6295.

(17) Amara, A., Gall, S. L., Schwartz, O., Salamero, J., Montes, M., Loetscher, P., Baggiolini, M., Virelizier, J. L., and Arenzana-Seisdedos, F. (1997) HIV coreceptor downregulation as antiviral principle: SDF-1alpha-dependent internalization of the chemokine receptor CXCR4 contributes to inhibition of HIV replication. *J. Exp. Med. 186*, 139−146.

(18) Altenburg, J. D., Jin, Q., Alkhatib, B., and Alkhatib, G.. (2010) The potent anti-HIV activity of CXCL12γ correlates with efficient CXCR4 binding and internalization. *J. Virol. 84*, 2563−2572.

(19) Tamamura, H., Xu, Y., Hattori, T., Zhang, X., Arakaki, R., Kanbara., K., Omagari, A., Otaka, A., Ibuka, T., Yamamoto, N., Nakashima, H., and Fujii, N. (1998) A low-molecular-weight inhibitor against the chemokine receptor CXCR4: a strong anti-HIV peptide T140. *Biochem. Biophys. Res. Commun. 253*, 877−882.

(20) Gerlach, L. O., Skerlj, R. T., Bridger, G. J., and Schwartz, T. W. (2001) Molecular interactions of cyclam and bicyclam non-peptide antagonists with the CXCR4 chemokine receptor. *J. Biol. Chem. 276*, 14153−14160.

(21) Oishi, S., Masuda, R., Evans, B., Ueda, S., Goto, Y., Ohno, H., Hirasawa, A., Tsujimoto, G., Wang, Z., Peiper, S. C., Naito, T., Kodama, E., Matsuoka, M., and Fujii, N. (2008) Synthesis and application of fluorescein- and biotin-labeled molecular probes for the chemokine receptor CXCR4. *ChemBioChem 9*, 1154−1158.

(22) Masuda, R., Oishi, S., Ohno, H., Kimura, H., Saji, H., and Fujii, N. (2011) Concise site-specific synthesis of DTPA-peptide conjugates: application to imaging probes for the chemokine receptor CXCR4. *Bioorg. Med. Chem. 19*, 3216−3220.

(23) Zhang, W. B., Navenot, J. M., Haribabu, B., Tamamura, H., Hiramatu, K., Omagari, A., Pei, G., Manfredi, J. P., Fujii, N., Broach, J. R., and Peiper, S. C. (2002) A point mutation that confers constitutive activity to CXCR4 reveals that T140 is an inverse agonist and that AMD3100 and ALX40−4C are weak partial agonists. *J. Biol. Chem. 277*, 24515−24521.

(24) Wu, B., Chien, E. Y., Mol, C. D., Fenalti, G., Liu, W., Katritch, V., Abagyan, R., Brooun, A., Wells, P., Bi, F. C., Hamel, D. J., Kuhn, P., Handel, T. M., Cherezov, V., and Stevens, R. C. (2010) Structures of the CXCR4 chemokine GPCR with small-molecule and cyclic peptide antagonists. *Science 330*, 1066−1071.

(25) Crump, M. P., Gong, J. H., Loetscher, P., Rajarathnam, K., Amara, A., Arenzana-Seisdedos, F., Virelizier, J. L., Baggiolini, M., Sykes, B. D., and Clark-Lewis, I. (1997) Solution structure and basis for functional activity of stromal cell-derived factor-1; dissociation of CXCR4 activation from binding and inhibition of HIV-1. *EMBO J. 16*, 6996−7007.

(26) Trent, J. O., Wang, Z. X., Murray, J. L., Shao, W., Tamamura, H., Fujii, N., and Peiper, S. C. (2003) Lipid bilayer simulations of CXCR4 with inverse agonists and weak partial agonists. *J. Biol. Chem. 278*, 47136−47144.

(27) Doranz, B. J., Grovit-Ferbas, K., Sharron, M. P., Mao, S. H., Goetz, M. B., Daar, E. S., Doms, R. W., and O'Brien, W. A. (1997) A small-molecule inhibitor directed against the chemokine receptor CXCR4 prevents its use as an HIV-1 coreceptor. *J. Exp. Med. 186*, 1395−1400.

(28) Futaki, S., Nakase, I., Tadokoro, A., Takeuchi, T., and Jones, A. T. (2007) Arginine-rich peptides and their internalization mechanisms. *Biochem. Soc. Trans. 35*, 784−787.

(29) Nakase, I., Tadokoro, A., Kawabata, N., Takeuchi, T., Katoh, H., Hiramoto, K., Negishi, M., Nomizu, M., Sugiura, Y., and Futaki, S. (2007) Interaction of arginine-rich peptides with membrane-associated proteoglycans is crucial for induction of actin organization and macropinocytosis. *Biochemistry 46*, 492−501.
(30) Fuchs, S. M., and Raines, R. T. (2004) Pathway for polyarginine entry into mammalian cells. *Biochemistry 9*, 2438−2444.
(31) Jones, S. W., Christison, R., Bundell, K., Voyce, C. J., Brockbank, S. M., Newham, P., and Lindsay, M. A. (2005) Characterisation of cell-penetrating peptide-mediated peptide delivery. *Br. J. Pharmacol. 145*, 1093−1102.
(32) Yano, Y., Yano, A., Oishi, S., Sugimoto, Y., Tsujimoto, G., Fujii, N., and Matsuzaki, K. (2008) Coiled-coil tag--probe system for quick labeling of membrane receptors in living cell. *ACS Chem. Biol. 3*, 341−345.
(33) Zhang, Y., Foudi, A., Geay, J. F., Berthebaud, M., Buet, D., Jarrier, P., Jalil, A., Vainchenker, W., and Louache, F. (2004) Intracellular localization and constitutive endocytosis of CXCR4 in human CD34+ hematopoietic progenitor cells. *Stem Cells 22*, 1015−1029.
(34) Hesselgesser, J., Liang, M., Hoxie, J., Greenberg, M., Brass, L. F., Orsini, M. J., Taub, D., and Horuk, R. (1998) Identification and characterization of the CXCR4 chemokine receptor in human T cell lines: ligand binding, biological activity, and HIV-1 infectivity. *J. Immunol. 160*, 877−883.
(35) Honczarenko, M., Douglas, R. S., Mathias, C., Lee, B., Ratajczak, M. Z., and Silberstein, L. E. (1999) SDF-1 responsiveness does not correlate with CXCR4 expression levels of developing human bone marrow B cells. *Blood 94*, 2990−2998.
(36) Masuda, R.; Oishi, S.; Tanahara, N.; Ohno, H.; Hirasawa, A.; Tsujimoto, G.; Kodama, E.; Matsuoka, M.; Fujii, N. Development and application of fluorescent SDF-1 derivatives. *Future Med. Chem.* **2012**, in press.
(37) Tamamura, H., Hiramatsu, K., Mizumoto, M., Ueda, S., Kusano, S., Terakubo, S., Akamatsu, M., Yamamoto, N., Trent, J. O., Wang, Z., Peiper, S. C., Nakashima, H., Otaka, A., and Fujii, N. (2003) Enhancement of the T140-based pharmacophores leads to the development of more potent and bio-stable CXCR4 antagonists. *Org. Biomol. Chem. 1*, 3663−3669.
(38) Fujii, N., Oishi, S., Hiramatsu, K., Araki, T., Ueda, S., Tamamura, H., Otaka, A., Kusano, S., Terakubo, S., Nakashima, H., Broach, J. A., Trent, J. O., Wang, Z. X., and Peiper, S. C. (2003) Molecular-size reduction of a potent CXCR4-chemokine antagonist using orthogonal combination of conformation- and sequence-based libraries. *Angew. Chem., Int. Ed. 42*, 3251−3253.
(39) Partial CXCR4 internalization was induced even by 1 nM TF14016, which was consistent with the potent bioactivity for CXCR4 as reported.[37]
(40) Vida, T. A, and Emr, S. D. (1995) A new vital stain for visualizing vacuolar membrane dynamics and endocytosis in yeast. *J. Cell. Biol. 128*, 779−792.
(41) Harvey, J. R., Mellor, P., Eldaly, H., Lennard, T. W., Kirby, J. A., and Ali, S. (2007) Inhibition of CXCR4-mediated breast cancer metastasis: a potential role for heparinoids? *Clin. Cancer Res. 13*, 1562−1570.
(42) Roettger, B. F., Ghanekar, D., Rao, R., Toledo, C., Yingling, J., Pinon, D., and Miller, L. J. (1997) Antagonist-stimulated internalization of the G protein-coupled cholecystokinin receptor. *Mol. Pharmacol. 51*, 357−362.
(43) Gray, J. A., and Roth, B. L. (2001) Paradoxical trafficking and regulation of 5-HT(2A) receptors by agonists and antagonists. *Brain Res. Bull. 56*, 441−451.
(44) Pheng, L. H., Dumont, Y., Fournier, A., Chabot, J. G., Beaudet, A., and Quirion, R. (2003) Agonist- and antagonist-induced sequestration/internalization of neuropeptide Y Y1 receptors in HEK293 cells. *Br. J. Pharmacol. 139*, 695−704.

Biochemical and Biophysical Research Communications 424 (2012) 257–261

Contents lists available at SciVerse ScienceDirect

Biochemical and Biophysical Research Communications

journal homepage: www.elsevier.com/locate/ybbrc

A simple, rapid, and sensitive system for the evaluation of anti-viral drugs in rats

Xiaoguang Li [a,b,f], Hua Qian [a,f], Fusako Miyamoto [a], Takeshi Naito [c], Kumi Kawaji [a], Kazumi Kajiwara [d,e], Toshio Hattori [a], Masao Matsuoka [c], Kentaro Watanabe [d], Shinya Oishi [d], Nobutaka Fujii [d], Eiichi N. Kodama [a,c,*]

[a] Tohoku University Graduate School of Medicine, Department of Internal Medicine/Division of Emerging Infectious Diseases, Sendai 980-8575, Japan
[b] Department of Medical Microbiology, Harbin Medical University, Harbin 150086, China
[c] Laboratory of Virus Control, Institute for Virus Research, Kyoto University, 53 Kawaramachi, Shogoin, Sakyo-ku, Kyoto 606-8507, Japan
[d] Graduate School of Pharmaceutical Sciences, Kyoto University, Sakyo-ku, Kyoto 606-8501, Japan
[e] JST Innovation Plaza Kyoto, Japan Science and Technology Agency, Nishigyo-ku, Kyoto 615-8245, Japan
[f] Center for AIDS Research, Kumamoto University, 2-2-1 Honjo, Kumamoto 860-0811, Japan

ARTICLE INFO

Article history:
Received 6 June 2012
Available online 23 June 2012

Keywords:
HIV-1
MAGI assay
Rat
CXCR4 antagonist
Fusion inhibitor

ABSTRACT

The lack of small animal models for the evaluation of anti-human immunodeficiency virus type 1 (HIV-1) agents hampers drug development. Here, we describe the establishment of a simple and rapid evaluation system in a rat model without animal infection facilities. After intraperitoneal administration of test drugs to rats, antiviral activity in the sera was examined by the MAGI assay. Recently developed inhibitors for HIV-1 entry, two CXCR4 antagonists, TF14016 and FC131, and four fusion inhibitors, T-20, T-20EK, SC29EK, and TRI-1144, were evaluated using HIV-1_{IIIB} and HIV-1_{BaL} as representative CXCR4- and CCR5-tropic HIV-1 strains, respectively. CXCR4 antagonists were shown to only possess anti-HIV-1_{IIIB} activity, whereas fusion inhibitors showed both anti-HIV-1_{IIIB} and anti-HIV-1_{BaL} activities in rat sera. These results indicate that test drugs were successfully processed into the rat sera and could be detected by the MAGI assay. In this system, TRI-1144 showed the most potent and sustained antiviral activity. Sera from animals not administered drugs showed substantial anti-HIV-1 activity, indicating that relatively high dose or activity of the test drugs might be needed. In conclusion, the novel rat system established here, "phenotypic drug evaluation", may be applicable for the evaluation of various antiviral drugs *in vivo*.

1. Introduction

Numerous antiviral agents have been developed to suppress infection with viruses such as human immunodeficiency virus type 1 (HIV-1) [1], and have successfully provided excellent outcomes *in vivo*. However, the emergence of drug-resistant HIV-1 variants is a major concern in HIV therapy. Therefore, the development of novel drugs with sustained activity to resistant variants is desirable. Drugs, especially those targeting HIV-1 entry, have been recently developed and approved, such as a CCR5 antagonist, maraviroc [2], and a fusion inhibitor, enfuvirtide (T-20) [3], where both drugs effectively suppress HIV-1 in the patient even resistant to previous drugs [4,5].

In addition to CCR5, which is a main co-receptor for clinical HIV-1 strains, CXCR4 can also act as a co-receptor for HIV-1 (X4-tropic HIV-1), such as that seen for the vast majority of laboratory-adapted HIV-1 strains [6]. Thus, CXCR4 is also considered an important therapeutic target. We previously identified a β-sheet-like 14-residue peptide, T140 [7,8], and its down-sized analog, a cyclic pentapeptide FC131 (Fig. 1) [9], as potent and specific CXCR4 antagonists. Both T140 and FC131 were proved to inhibit X4-tropic HIV-1 infection *in vitro*. T140 has been further modified to TF14016 (4F-benzoyl-TN14003; BKT140) that shows more potent inhibitory effect [10].

The first fusion inhibitor, T-20, efficiently inhibits replication of HIV-1 resistant even to inhibitors for reverse transcriptase and protease [11,12]. However, the genetic barrier to overcome suppression by T-20 seems to not be high since a 1–2 amino acid(s) substitution in gp41 appears to be sufficient for resistance [13–15]. Therefore, we developed T-20EK [16] and SC29EK [17] as novel and potent fusion inhibitors that sustain their inhibitory effects on T-20 resistant HIV-1 stains. A series of systematic replacements with hydrophilic glutamic acid (E) or lysine (K) was introduced (EK motif) at the solvent-accessible site to enhance the α-helicity of the peptides by possible intrahelical electrostatic interactions [18]. T-20EK/S138A [16] was synthesized

* Corresponding author at: Tohoku University Graduate School of Medicine, Department of Internal Medicine/Division of Emerging Infectious Diseases, Building 1 Room 515, 2-1 Seiryo cho, Aoba-ku, Sendai 980-8575, Japan. Fax: +81 22 717 8221.
E-mail addresses: kodama515@med.tohoku.ac.jp, kodausa21@gmail.com (E.N. Kodama).

0006-291X/$ - see front matter © 2012 Elsevier Inc. All rights reserved.
http://dx.doi.org/10.1016/j.bbrc.2012.06.097

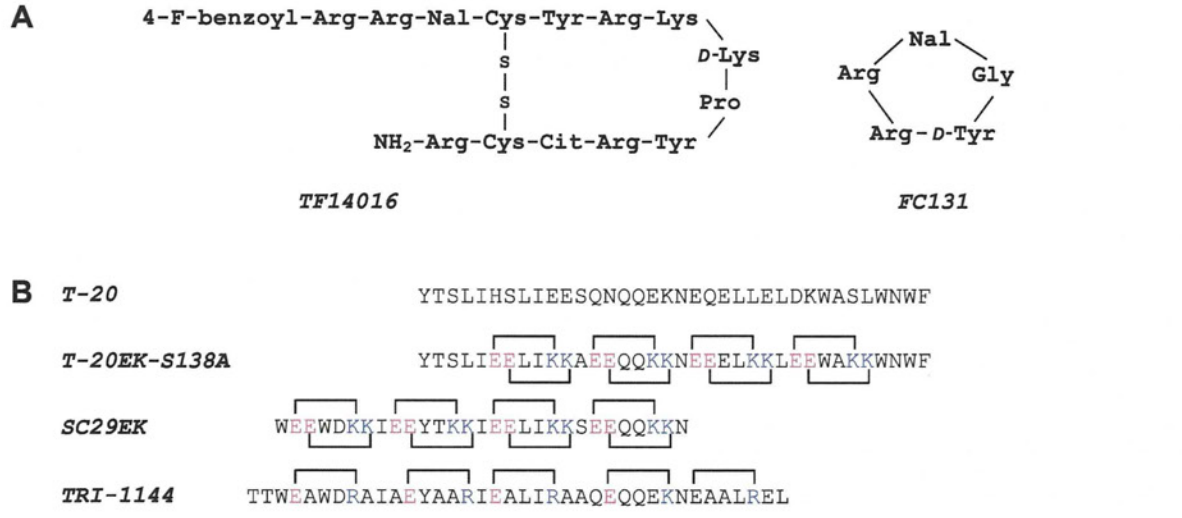

Fig. 1. Amino acid sequences of peptide-based drugs. (A) CXCR4 antagonists used in this study are shown. Nal: L-3-(2-naphthyl)alanine; Cit: L-citrulline. (B) Fusion inhibitors used are shown. T-20 is original sequenced of gp41 C-HR region. Electrostatic interactions are indicated by the linker. SC29EK and T-20EK/S138A, contain EExxKKx motif, while TRI-1144 does ExxxRxx motif. x indicates original and/or modified amino acids. Each motif creates 2 and 1 interaction(s) in each helical turn. T-20 resistance associated mutation, S138A, is introduced into T-20EK sequence (T-20EK/S138A). All peptides are N-terminally acetylated and C-terminally amidated.

with a combined rational design by the introduction of the EK motif for enhancement of α-helicity and increased affinity to mutated gp41 by S138A, a T-20 resistant associated mutation [19]. Dwyer et al. developed another fusion inhibitor, TRI-1144 (T-2635) that also exerted potent activity against T-20 resistant variants [20,21]. The amino acid sequence of TRI-1144 is also modified by substitutions with E and arginine (R), similar to the EK motif introduced into T-20EK and SC29EK.

Analyses of the efficacy and adverse effects of new drugs in animal models are important prior to their clinical application. Indeed, generally, the toxic effects, kinetics, and efficacy of new drugs are expected to be obtained by animal experiments. In the case of anti-HIV-1 drugs, the toxic effects of drug candidates can be determined by animal experiments. Furthermore, the kinetics of some drugs may be examined by some analytical methods such as liquid chromatography–mass spectrometry (LC–MS) [22] or bioimaging with labeled compounds. Unfortunately, these results may not be well-correlated with *in vivo* efficacy due to degradation and/or modification of drugs, and the detection of false positives of similar component(s) *in vivo* [23]. The efficacy of anti-HIV-1 drugs is, so far, hard to examine *in vivo* due to the lack of convenient animal infection models with low cost. One of the main obstacles to establish appropriate animal models is restricted infection of small animals with HIV-1, such as for mice, rats, and ferrets. An HIV-1 receptor-transgenic rat model has been developed for the analysis of HIV-1 infection *in vivo*; however, the levels of plasma viremia in infected rats were modest and not sustained [24,25]. Monkeys infected with simian immunodeficiency virus-HIV chimeric virus (SHIV) is the only model for the evaluation of HIV-1 replication [26], but comes at a high cost, especially for animal infection facilities. Taken together, novel rapid, simple, and sensitive HIV-1 infection models with low cost, such as those in small animals, are urgently needed to be established.

Here, we established a new system to evaluate the anti-HIV-1 activity of drugs and its kinetics in rats in addition to their toxic effects. The bioavailability of anti-HIV-1 drugs in sera was determined for the assessment of antiviral activity *in vitro*. The *in vivo* efficacy of various peptide-based entry inhibitors, such as TF14016, FC131, T-20EK/S138A, SC29EK, and TRI-1144, were assessed using this model and may be useful for the *in vivo* assessment of novel entry inhibitors.

2. Materials and methods

2.1. Drugs and cells

CXCR4 antagonists, TF14016 and FC131, and fusion inhibitors, T-20, T-20EK/S138A, SC29EK and TRI1144, were synthesized as previously described [7,9,16–18,20]. For *in vitro* drug susceptibility assays and *in vivo* administration, the test drugs were dissolved in 50% dimethyl sulfoxide (DMSO; 2 mM) and sterile water (3 or 10 mg/1.5 mL), respectively. MAGI CCR5 cells (HeLa CD4/CCR5/LTR-β-galactosidase cells) were obtained through the NIH AIDS Research and Reference Reagent Program, Division of AIDS, NIAID: from Dr. Julie Overbaugh [27–29] and were maintained in Dulbecco's modified Eagle's medium (DMEM) supplemented with 10% fetal calf serum [30].

2.2. Administration of drugs

Animal experiments were performed in the Biotechnical Center of the Japan SLC, in accordance with the institutional ethical guidelines. To examine the pharmacological kinetics in sera, rats were used for collection of sera. Drugs were used at 3 mg/1.5 mL/kg of T-20, 3 mg/1.5 mL/kg of TF14016, 10 mg/1.5 mL/kg of FC131, 10 mg/1.5 mL/kg of SC29EK, 10 mg/1.5 mL/kg of T-20EK/S138A, and 3 mg/1.5 mL/kg of TRI1144, and were intraperitoneally administrated to six groups of six male SD rats (7 weeks). Sera were then harvested 0.5, 1, 2, 4, 8, and 12 h from the administrated rat, and stored at −80 °C.

2.3. MAGI assay

The anti-HIV-1 activity of drugs in rat sera after drug administration was detected by the MAGI assay, as previously described [31]. Briefly, MAGI CCR5 cells were transferred to 96-well plates at 1×10^4 cells per well. On the following day, serially-diluted drugs or rat sera were added to cells in triplicate with HIV-1 preparations (HIV-1_{IIIB} or HIV-1_{BaL}). After 48 h, cultured cells were fixed with 1% (v/v) formaldehyde and 0.2% (v/v) glutaraldehyde in phosphate-buffered saline (PBS), and were stained with 0.4 mg/mL 5-bromo-4-chloro-3-indolyl-2-D-galactopyranoside (X-gal). Blue

cells were counted by observation under a light microscope. The 50% effective concentration was defined as the serum dilution fold or drug concentration that inhibited virus infection in 50% of the wells.

3. Results

3.1. Anti-HIV-1 activity of drugs in vitro

Prior to animal experiments, the anti-HIV-1 activity of test drugs *in vitro* was determined by the MAGI assay. HIV-1_{IIIB} and HIV-1_{BaL} were used as representative X4- and R5-tropic HIV-1 strains, respectively. TF14016 exerted most potent anti-HIV-1 activity *in vitro* compared to other inhibitors as shown in Table 1. As expected, the two CXCR4 antagonists, TF14016 and FC131, inhibited replication of only HIV-1_{IIIB}, but not HIV-1_{BaL}, which uses CCR5 for its entry. All four fusion inhibitors, T-20EK/S138A, SC29EK, TRI-1144 and T-20, comparably inhibited replication of both HIV-1_{IIIB} and HIV-1_{BaL}. Among newly developed fusion inhibitors, T-20EK/S138A showed the strongest inhibitory effect both on HIV-1_{IIIB} and HIV-1_{BaL}. Our antiviral data are similar to previous observations for TF14016 and FC131 [7–10,32], T-20EK/S138A [16], SC29EK [17], and TRI-1144 [20,21].

3.2. Anti-HIV-1 activity of CXCR4 antagonists in rat

First, we examined background anti-HIV-1 activity in four PBS-injected rat sera as negative controls. In the control rat sera, anti-HIV-1_{IIIB} and HIV-1_{BaL} activities were detected (Fig. 2). Rat sera showed antiviral activity up to the 90- and 160-fold dilution for HIV-1_{IIIB} and HIV-1_{BaL} (Fig. 2; shown as a baseline activity).

The two CXCR4 antagonists, TF14016 and FC131, were intraperitoneally injected into six rats and sera were withdrawn at the indicated time as shown in Fig. 2. Drug activities were detected up to 4 h, with peak time point at 1 h after the administration. Surprisingly, sera from two rats injected with TF14016 and four rats with FC131 also weakly showed anti-HIV-1_{BaL} activity (data not shown). However, both CXCR4 antagonists were generally effective only against HIV-1_{IIIB}.

3.3. Anti-HIV-1 activity of fusion inhibitors in rat

Anti-HIV-1_{IIIB} and anti-HIV-1_{BaL} activities were detected in four rat sera and all six rat sera, respectively, that were administered T-20. Anti-HIV-1 activity of T-20 in rats was detected up to 8 h with a peak time point 1–2 h after administration. Anti-HIV-1_{IIIB} activities were detected in sera of six rats injected with SC29EK, T-20EK/S138A, and TRI-1144, which were detected up to 3, 8, and 8 h, respectively, with serum peak levels at 1–2 h after administration. Anti-HIV-1_{BaL} activities were detected in sera with SC29EK, T-20EK/S138A, and TRI-1144 with similar extent with these for HIV-1_{IIIB}. These results indicate that in rats, intraperitoneally injected drug activities were present in sera and may exert anti-HIV-1 activity *in vivo*. Among these, TRI-1144 showed stable and relatively sustained activity.

3.4. Effect of heat inactivation

To identify component(s) for baseline anti-HIV-1 activity in rat sera, we examined heat inactivation. As expected, non-specific anti-HIV-1 activity in sera decreased in a time-dependent manner. At 1000-fold dilution of sera, non-specific activity was completely abolished (Fig. 3); unfortunately the drugs tested in the study were not heat stable and irreversible even at 56 °C (data not shown). However, when administered a physiological dose, anti-HIV-1 activity was detectable even without heat inactivation (Fig. 2). Therefore, the rat model system proved to be adequate to evaluate the efficacy of drugs.

3.5. Toxic effect of drugs in rats

All peptides tested showed no apparent lethal effect at the administered dosages, except for FC131, where one rat succumbed from unknown causes at a dose of 30 mg/kg.

4. Discussion

To develop effective and safe antiviral agents, *in vitro* screening systems are established for some viruses, while *in vivo* evaluation systems using small animals are hampered by limited infection efficiency and the need for specialized facilities. In the case of animal models for HIV-1, animal models are largely restricted [33]. In the present study, we describe the establishment of a novel evaluation system of anti-HIV-1 drugs through *in vitro* detection of anti-HIV-1 activity in the sera of rats administrated drugs using the MAGI assay. The *in vivo* efficacies of five potential entry inhibitors were evaluated. In this system, only TRI-1144 consistently showed potent and sustained activity compared with T-20. The glutamic acid–arginine (ER) modification, but not the glutamic acid–lysine (EK) modification and/or alanine substitutions to the peptide (Fig. 1), may have beneficial effects on stability and efficacy, resulting in sustained anti-HIV-1 activities. The simple and convenient *in vivo* efficacy evaluation system established in this study not only reveals whether drugs exert anti-HIV-1 activity *in vivo*, but also provides *in vivo* kinetics without the need for infectious animal facilities. Moreover, this system can be used for the evaluation of not only anti-HIV-1 drugs *in vivo*, but also of drugs against other viruses *in vivo*. Nonetheless, the sera produced by the rats can be also applied to resistant virus variants and clinical isolates resulting in a reduction of the number animal experiments required.

Other methods, such as a high performance liquid chromatography (HPLC), may provide accurate measurement of the drug concentration in sera and was performed in this study. Even after administration of FC131 at 30 mg/kg, we could only detect FC131 at the peak concentration (data not shown). In a case of small amount of agents with extremely high activity, it is possible to fail to detect by HPLC. For more sensitive detection by HPLC, further labeling, such as with radioisotopes, may be needed. In addition, HPLC analysis can detect drugs that have been modified and/or degraded by *in vivo* metabolism when they are spectrometrically indistinguishable. However, our system detects only the active

Table 1
Anti-HIV-1 activity of drugs *in vitro*.

Virus	EC_{50}[a] (nM)					
	TF14016	FC131	T-20	T-20EK/S138A	SC29EK	TRI-1144
HIV-1_{IIIB}	0.3 ± 0.0	17.4 ± 5.7	42.3 ± 7.6	2.0 ± 0.5	8.3 ± 1.3	4.6 ± 0.6
HIV-1_{BaL}	>10,000	>10,000	16.2 ± 4.9	0.4 ± 0.2	1.4 ± 0.2	0.4 ± 0.2

[a] Antiviral activity, shown as EC_{50}, was determined using the MAGI assay. Each EC_{50} represents the mean ± SD obtained from at least three independent experiments. HIV-1_{IIIB} and HIV-1_{BaL} were used as representative X4 and R5 HIV-1 strains, respectively.

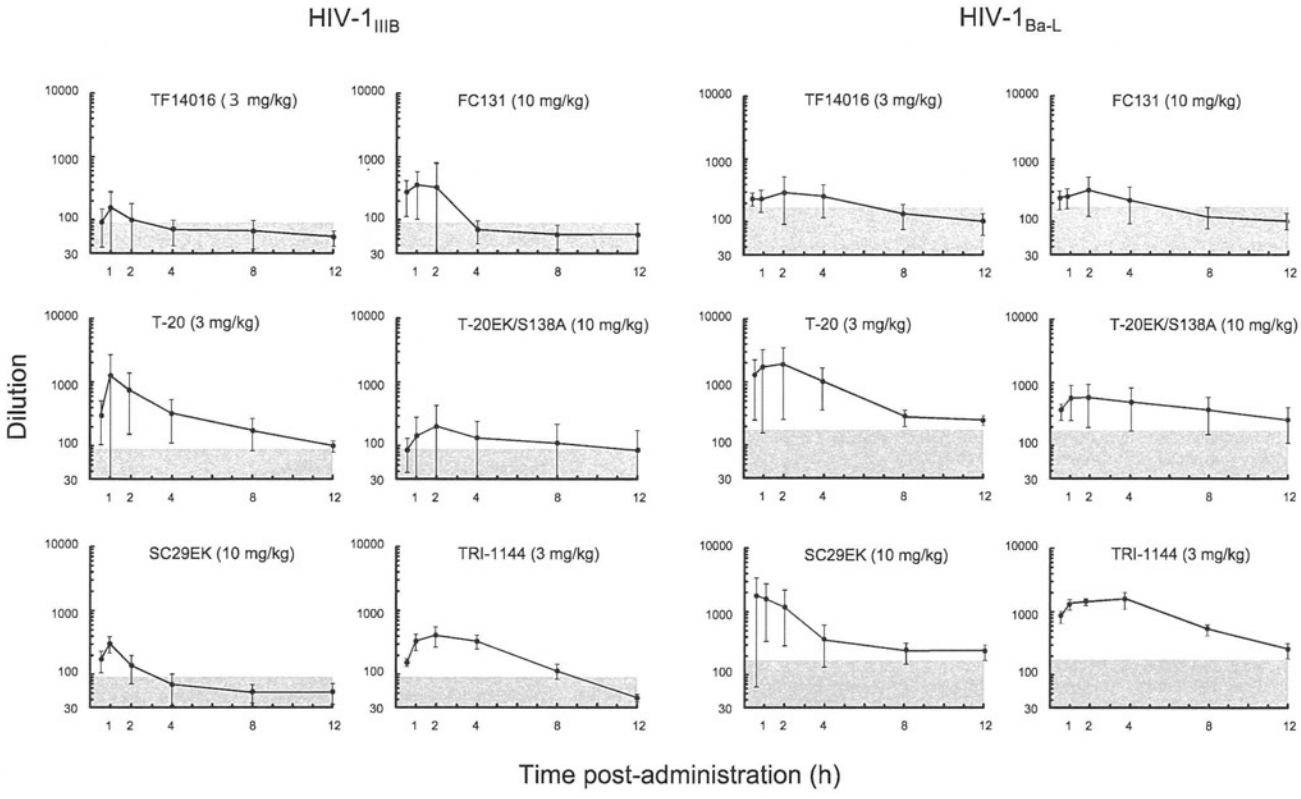

Fig. 2. Anti-HIV-1 activity of drugs *in vivo*. Six groups of six rats were administered each drug by intra-peritoneal injection and rat sera were harvested at different time points post-administration. All serum samples were analyzed by MAGI assay for 50% inhibition of infections of HIV-1_{IIIB} and HIV-1_{BaL}. This experiment was performed in triplicate for each rat. Data represent mean ± SD of from six rats. Gray shade indicates average results of age-matched rat sera as negative controls.

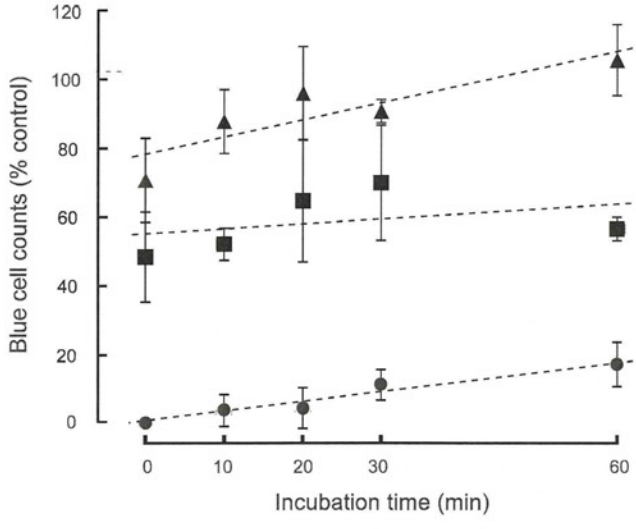

Fig. 3. Heat inactivation of sera. Rat sera without heat activation were examined using the MAGI assay. Heat inactivation was performed at 56 °C. Ten-fold dilutions of sera were resistant to heat inactivation even after 1 h inactivation (~20%). At the 1000-fold dilution, most of the inherent inhibitory effect was removed.

form of the agents, and in addition provides direct comparison of the tested drugs *in vitro* and *in vivo*, since the assay utilizes identical evaluation by the MAGI assay. In comparison, the rat *in vitro* system revealed that TRI-1144 showed strong and sustained activity compared with T-20EK/S138A and SC29EK. In this study, we only performed intraperitoneal injection that may have an effect on drug metabolism(s). Further experiments, such as subcutaneous injection, for which TF14016 shows greater efficacy [34,35], should be performed and compared with other administration roots.

The two CXCR4 antagonists analyzed in this study, TF14016 and FC131, showed moderate anti-HIV-1_{BaL} activity *in vivo*, and sera from two rats administered T-20 inhibited HIV-1 infection less efficiently (data not shown). These unexpected data might result from the relatively high background caused by non-specific inhibitory component(s) in sera. As shown in Fig. 2, sera from rats not administered drugs also showed moderate anti-HIV-1_{IIIB} and anti-HIV-1_{BaL} activities. Therefore, the development of a reagent or method for removal of background activity in rat sera may improve the accuracy and sensitivity of this *in vivo* drug efficacy evaluation method. For instance, serum albumin [36], lactoferrin [37,38], and transferrin [39] may influence HIV replication. Unfortunately, the drugs used in this study were all peptide-derived agents, therefore, heat-inactivation may reduce antiviral activity. Therefore, administration of relatively high doses of drug may be required to overcome this inhibition.

In conclusion, we established a novel, simple and rapid system for the phenotypic evaluation of anti-HIV-1 drugs in a rat model. This system may also be applicable for the analysis of other antiviral drugs for viruses that do not have an appropriate infection model in rodents, and/or useful for the initial screening, such for dosing, administration root decision and other factors, prior to actual animal infection experiments. In this system for HIV infection, TRI-1144 displayed the most potent anti-HIV-1 activity *in vivo* of the six drugs analyzed.

Acknowledgments

This work was supported by a Grant from the Ministry of Education, Culture, Sports, Science, and Technology of Japan, a Grant

for the Promotion of AIDS Research from the Ministry of Health, Labour and Welfare, a Grant for Research for Health Sciences Focusing on Drug Innovation from the Japan Health Sciences Foundation and the Science and Technology Incubation Program in Advanced Regions from the Japan Science and Technology Agency.

References

[1] E. De Clercq, Antiretroviral drugs, Curr. Opin. Pharmacol. 10 (2010) 507–515.
[2] P. Dorr, M. Westby, S. Dobbs, P. Griffin, B. Irvine, M. Macartney, J. Mori, G. Rickett, C. Smith-Burchnell, C. Napier, R. Webster, D. Armour, D. Price, B. Stammen, A. Wood, M. Perros, Maraviroc (UK-427,857), a potent, orally bioavailable, and selective small-molecule inhibitor of chemokine receptor CCR5 with broad-spectrum anti-human immunodeficiency virus type 1 activity, Antimicrob. Agents Chemother. 49 (2005) 4721–4732.
[3] C.T. Wild, D.C. Shugars, T.K. Greenwell, C.B. McDanal, T.J. Matthews, Peptides corresponding to a predictive alpha-helical domain of human immunodeficiency virus type 1 gp41 are potent inhibitors of virus infection, Proc. Natl. Acad. Sci. USA 91 (1994) 9770–9774.
[4] G. Fatkenheuer, A.L. Pozniak, M.A. Johnson, A. Plettenberg, S. Staszewski, A.I. Hoepelman, M.S. Saag, F.D. Goebel, J.K. Rockstroh, B.J. Dezube, T.M. Jenkins, C. Medhurst, J.F. Sullivan, C. Ridgway, S. Abel, I.T. James, M. Youle, E. van der Ryst, Efficacy of short-term monotherapy with maraviroc, a new CCR5 antagonist, in patients infected with HIV-1, Nat. Med. 11 (2005) 1170–1172.
[5] J.P. Lalezari, K. Henry, M. O'Hearn, J.S. Montaner, P.J. Piliero, B. Trottier, S. Walmsley, C. Cohen, D.R. Kuritzkes, J.J. Eron Jr., J. Chung, R. DeMasi, L. Donatacci, C. Drobnes, J. Delehanty, M. Salgo, Enfuvirtide, an HIV-1 fusion inhibitor, for drug-resistant HIV infection in North and South America, N. Engl. J. Med. 348 (2003) 2175–2185.
[6] Y. Feng, C.C. Broder, P.E. Kennedy, E.A. Berger, HIV-1 entry cofactor: functional cDNA cloning of a seven-transmembrane, G protein-coupled receptor, Science 272 (1996) 872–877.
[7] H. Tamamura, A. Omagari, S. Oishi, T. Kanamoto, N. Yamamoto, S.C. Peiper, H. Nakashima, A. Otaka, N. Fujii, Pharmacophore identification of a specific CXCR4 inhibitor, T140, leads to development of effective anti-HIV agents with very high selectivity indexes, Bioorg. Med. Chem. Lett. 10 (2000) 2633–2637.
[8] H. Tamamura, Y. Xu, T. Hattori, X. Zhang, R. Arakaki, K. Kanbara, A. Omagari, A. Otaka, T. Ibuka, N. Yamamoto, H. Nakashima, N. Fujii, A low-molecular-weight inhibitor against the chemokine receptor CXCR4: a strong anti-HIV peptide T140, Biochem. Biophys. Res. Commun. 253 (1998) 877–882.
[9] N. Fujii, S. Oishi, K. Hiramatsu, T. Araki, S. Ueda, H. Tamamura, A. Otaka, S. Kusano, S. Terakubo, H. Nakashima, J.A. Broach, J.O. Trent, Z.X. Wang, S.C. Peiper, Molecular-size reduction of a potent CXCR4-chemokine antagonist using orthogonal combination of conformation- and sequence-based libraries, Angew. Chem. Int. Ed. Engl. 42 (2003) 3251–3253.
[10] H. Tamamura, K. Hiramatsu, M. Mizumoto, S. Ueda, S. Kusano, S. Terakubo, M. Akamatsu, N. Yamamoto, J.O. Trent, Z. Wang, S.C. Peiper, H. Nakashima, A. Otaka, N. Fujii, Enhancement of the T140-based pharmacophores leads to the development of more potent and bio-stable CXCR4 antagonists, Org. Biomol. Chem. 1 (2003) 3663–3669.
[11] J.P. Lalezari, K. Henry, M. O'Hearn, J.S. Montaner, P.J. Piliero, B. Trottier, S. Walmsley, C. Cohen, D.R. Kuritzkes, J.J. Eron, J. Chung, R. DeMasi, L. Donatacci, C. Drobnes, J. Delehanty, M. Salgo, T.S. Group, Enfuvirtide, an HIV-1 fusion inhibitor, for drug-resistant HIV infection in North and South America, N. Engl. J. Med. 348 (2003) 2175–2185.
[12] A. Lazzarin, B. Clotet, D. Cooper, J. Reynes, K. Arasteh, M. Nelson, C. Katlama, H.J. Stellbrink, J.F. Delfraissy, J. Lange, L. Huson, R. DeMasi, C. Wat, J. Delehanty, C. Drobnes, M. Salgo, T.S. Group, Efficacy of enfuvirtide in patients infected with drug-resistant HIV-1 in Europe and Australia, N. Engl. J. Med. 348 (2003) 2186–2195.
[13] B. Labrosse, L. Morand-Joubert, A. Goubard, S. Rochas, J.L. Labernardière, J. Pacanowski, J.L. Meynard, A.J. Hance, F. Clavel, F. Mammano, Role of the envelope genetic context in the development of enfuvirtide resistance in human immunodeficiency virus type 1-infected patients, J. Virol. 80 (2006) 8807–8819.
[14] E. Poveda, B. Rodés, C. Toro, L. Martín-Carbonero, J. Gonzalez-Lahoz, V. Soriano, Evolution of the gp41 env region in HIV-infected patients receiving T-20, a fusion inhibitor, AIDS 16 (2002) 1959–1961.
[15] B. Zöllner, H.H. Feucht, M. Schröter, P. Schäfer, A. Plettenberg, A. Stoehr, R. Laufs, Primary genotypic resistance of HIV-1 to the fusion inhibitor T-20 in long-term infected patients, AIDS 15 (2001) 935–936.
[16] S. Oishi, S. Ito, H. Nishikawa, K. Watanabe, M. Tanaka, H. Ohno, K. Izumi, Y. Sakagami, E. Kodama, M. Matsuoka, N. Fujii, Design of a novel HIV-1 fusion inhibitor that displays a minimal interface for binding affinity, J. Med. Chem. 51 (2008) 388–391.
[17] T. Naito, K. Izumi, E. Kodama, Y. Sakagami, K. Kajiwara, H. Nishikawa, K. Watanabe, S.G. Sarafianos, S. Oishi, N. Fujii, M. Matsuoka, SC29EK, a peptide fusion inhibitor with enhanced alpha-helicity, inhibits replication of human immunodeficiency virus type 1 mutants resistant to enfuvirtide, Antimicrob. Agents Chemother. 53 (2009) 1013–1018.
[18] H. Nishikawa, S. Oishi, M. Fujita, K. Watanabe, R. Tokiwa, H. Ohno, E. Kodama, K. Izumi, K. Kajiwara, T. Naitoh, M. Matsuoka, A. Otaka, N. Fujii, Identification of minimal sequence for HIV-1 fusion inhibitors, Bioorg. Med. Chem. 16 (2008) 9184–9187.
[19] K. Izumi, E. Kodama, K. Shimura, Y. Sakagami, K. Watanabe, S. Ito, T. Watabe, Y. Terakawa, H. Nishikawa, S.G. Sarafianos, K. Kitaura, S. Oishi, N. Fujii, M. Matsuoka, Design of peptide-based inhibitors for human immunodeficiency virus type 1 strains resistant to T-20, J. Biol. Chem. (2009) 4914–4920.
[20] D.K. Davison, R.J. Medinas, S.M. Mosier, T.S. Bowling, M.K. Delmedico, J.J. Dwyer, N. Cammack, M.L. Greenberg, New fusion inhibitor peptides, TRI-999 and TRI-1144, are potent inhibitors of enfuvirtide and T-1249 resistant isolates. in: Program and Abstracts of the 16 th International AIDS Conference, August 13 -18, 2006,Toronto, Canada, Abstract THPE0021.
[21] J.J. Dwyer, K.L. Wilson, D.K. Davison, S.A. Freel, J.E. Seedorff, S.A. Wring, N.A. Tvermoes, T.J. Matthews, M.L. Greenberg, M.K. Delmedico, Design of helical, oligomeric HIV-1 fusion inhibitor peptides with potent activity against enfuvirtide-resistant virus, Proc. Natl. Acad. Sci. USA 104 (2007) 12772–12777.
[22] E.N. Fung, Z. Cai, T.C. Burnette, A.K. Sinhababu, Simultaneous determination of Ziagen and its phosphorylated metabolites by ion-pairing high-performance liquid chromatography–tandem mass spectrometry, J. Chromatogr. B Biomed. Sci. Appl. 754 (2001) 285–295.
[23] Z. Cai, E.N. Fung, A.K. Sinhababu, Capillary electrophoresis-ion trap mass spectrometry analysis of Ziagen and its phosphorylated metabolites, Electrophoresis 24 (2003) 3160–3164.
[24] C. Goffinet, I. Allespach, O.T. Keppler, HIV-susceptible transgenic rats allow rapid preclinical testing of antiviral compounds targeting virus entry or reverse transcription, Proc. Natl. Acad. Sci. USA 104 (2007) 1015–1020.
[25] O.T. Keppler, F.J. Welte, T.A. Ngo, P.S. Chin, K.S. Patton, C.L. Tsou, N.W. Abbey, M.E. Sharkey, R.M. Grant, Y. You, J.D. Scarborough, W. Ellmeier, D.R. Littman, M. Stevenson, I.F. Charo, B.G. Herndier, R.F. Speck, M.A. Goldsmith, Progress toward a human CD4/CCR5 transgenic rat model for de novo infection by human immunodeficiency virus type 1, J. Exp. Med. 195 (2002) 719–736.
[26] R. Shibata, A. Adachi, SIV/HIV recombinants and their use in studying biological properties, AIDS Res. Hum. Retroviruses 8 (1992) 403–409.
[27] B. Chackerian, E.M. Long, P.A. Luciw, J. Overbaugh, Human immunodeficiency virus type 1 coreceptors participate in postentry stages in the virus replication cycle and function in simian immunodeficiency virus infection, J. Virol. 71 (1997) 3932–3939.
[28] J. Kimpton, M. Emerman, Detection of replication-competent and pseudotyped human immunodeficiency virus with a sensitive cell line on the basis of activation of an integrated beta-galactosidase gene, J. Virol. 66 (1992) 2232–2239.
[29] H. Deng, R. Liu, W. Ellmeier, S. Choe, D. Unutmaz, M. Burkhart, P. Di Marzio, S. Marmon, R.E. Sutton, C.M. Hill, C.B. Davis, S.C. Peiper, T.J. Schall, D.R. Littman, N.R. Landau, Identification of a major co-receptor for primary isolates of HIV-1, Nature 381 (1996) 661–666.
[30] E.I. Kodama, S. Kohgo, K. Kitano, H. Machida, H. Gatanaga, S. Shigeta, M. Matsuoka, H. Ohrui, H. Mitsuya, 4′-Ethynyl nucleoside analogs: potent inhibitors of multidrug-resistant human immunodeficiency virus variants *in vitro*, Antimicrob. Agents Chemother. 45 (2001) 1539–1546.
[31] D. Nameki, E. Kodama, M. Ikeuchi, N. Mabuchi, A. Otaka, H. Tamamura, M. Ohno, N. Fujii, M. Matsuoka, Mutations conferring resistance to human immunodeficiency virus type 1 fusion inhibitors are restricted by gp41 and Rev-responsive element functions, J. Virol. 79 (2005) 764–770.
[32] H. Tamamura, K. Hiramatsu, S. Ueda, Z. Wang, S. Kusano, S. Terakubo, J.O. Trent, S.C. Peiper, N. Yamamoto, H. Nakashima, A. Otaka, N. Fujii, Stereoselective synthesis of [L-Arg-L/D-3-(2-naphthyl)alanine]-type (E)-alkene dipeptide isosteres and its application to the synthesis and biological evaluation of pseudopeptide analogues of the CXCR4 antagonist FC131, J. Med. Chem. 48 (2005) 380–391.
[33] K.K. Van Rompay, Evaluation of antiretrovirals in animal models of HIV infection, Antiviral Res. 85 (2010) 159–175.
[34] K. Nishizawa, H. Nishiyama, Y. Matsui, T. Kobayashi, R. Saito, H. Kotani, H. Masutani, S. Oishi, Y. Toda, N. Fujii, J. Yodoi, O. Ogawa, Thioredoxin-interacting protein suppresses bladder carcinogenesis, Carcinogenesis 32 (2011) 1459–1466.
[35] T. Kitaori, H. Ito, E.M. Schwarz, R. Tsutsumi, H. Yoshitomi, S. Oishi, M. Nakano, N. Fujii, T. Nagasawa, T. Nakamura, Stromal cell-derived factor 1/CXCR4 signaling is critical for the recruitment of mesenchymal stem cells to the fracture site during skeletal repair in a mouse model, Arthritis Rheum. 60 (2009) 813–823.
[36] M.E. Kuipers, J.G. Huisman, P.J. Swart, M.P. de Béthune, R. Pauwels, H. Schuitemaker, E. De Clercq, D.K. Meijer, Mechanism of anti-HIV activity of negatively charged albumins: biomolecular interaction with the HIV-1 envelope protein gp120, J. Acquir. Immune Defic. Syndr. Hum. Retrovirol. 11 (1996) 419–429.
[37] F. Groot, T.B. Geijtenbeek, R.W. Sanders, C.E. Baldwin, M. Sanchez-Hernandez, R. Floris, Y. van Kooyk, E.C. de Jong, B. Berkhout, Lactoferrin prevents dendritic cell-mediated human immunodeficiency virus type 1 transmission by blocking the DC-SIGN–gp120 interaction, J. Virol. 79 (2005) 3009–3015.
[38] M.C. Harmsen, P.J. Swart, M.P. de Béthune, R. Pauwels, E. De Clercq, T.H. The, D.K. Meijer, Antiviral effects of plasma and milk proteins: lactoferrin shows potent activity against both human immunodeficiency virus and human cytomegalovirus replication *in vitro*, J. Infect. Dis. 172 (1995) 380–388.
[39] H. Drakesmith, A. Prentice, Viral infection and iron metabolism, Nat. Rev. Microbiol. 6 (2008) 541–552.

Organic & Biomolecular Chemistry

Dynamic Article Links

Cite this: *Org. Biomol. Chem.*, 2012, **10**, 6792

www.rsc.org/obc

PAPER

Concise synthesis and anti-HIV activity of pyrimido[1,2-*c*][1,3]benzothiazin-6-imines and related tricyclic heterocycles†

Tsukasa Mizuhara,[a] Shinya Oishi,*[a] Hiroaki Ohno,[a] Kazuya Shimura,[b] Masao Matsuoka[b] and Nobutaka Fujii*[a]

Received 11th May 2012, Accepted 22nd June 2012
DOI: 10.1039/c2ob25904d

3,4-Dihydro-2*H*,6*H*-pyrimido[1,2-*c*][1,3]benzothiazin-6-imine (PD 404182) is a virucidal heterocyclic compound active against various viruses, including HCV, HIV, and simian immunodeficiency virus. Using facile synthetic approaches that we developed for the synthesis of pyrimido[1,2-*c*][1,3]-benzothiazin-6-imines and related tricyclic derivatives, the parallel structural optimizations of the central 1,3-thiazin-2-imine core, the benzene part, and the cyclic amidine part of PD 404182 were investigated. Replacement of the 6-6-6 pyrimido[1,2-*c*][1,3]benzothiazin-6-imine framework with 5-6-6 or 6-6-5 derivatives led to a significant loss of anti-HIV activity, and introduction of a hydrophobic group at the 9- or 10-positions improved the potency. In addition, we demonstrated that the PD 404182 derivative exerts anti-HIV effects at an early stage of viral infection.

Introduction

Since azidothymidine (AZT), a nucleoside reverse transcriptase inhibitor (NRTI), was approved for the treatment of HIV infections, a number of anti-HIV drugs have been launched. For example, saquinavir and nevirapine were the first protease inhibitor and non-nucleoside reverse transcriptase inhibitor (NNRTI), respectively.[1] Highly active antiretroviral therapy (HAART) using a combination of these antiretrovirals is a standard treatment regimen for HIV infections. The HAART regimen significantly reduces viral load in infected patients, leading to significant therapeutic gains and reductions in morbidity and mortality.[2] However, long-term administration of multiple antiretrovirals to maintain life-long latent infection triggers the emergence of drug-resistant variants[3] and drug-related adverse effects.[4] For example, high-level viral resistance to NRTI such as AZT, stavudine, and didanosine is conferred by mutations frequently observed in patients with virologic failure on an NRTI-containing regimen.[5] In addition, lipodystrophy and metabolic disorders are often observed in patients receiving HIV protease inhibitors.[6] To overcome these problems, several antiretrovirals with new mechanisms of action have been developed in this decade. A peptide-based fusion inhibitor (enfuvirtide),[7] an integrase inhibitor (raltegravir),[8] and a CC chemokine receptor type 5 (CCR5) antagonist (maraviroc)[9] are examples of new molecular entities used as anti-HIV agents.

Recently, highly potent small-molecule anti-HIV agents have been reported, which bind to viral envelope proteins (Fig. 1). 2-Thioxo-1,3-thiazolidine derivative **1** shows potent inhibition of HIV-1 replication at nanomolar levels,[10] which are directed at the deep hydrophobic pocket in the N-terminal heptad repeat trimer of the viral gp41. Compound **1** blocks HIV-1-mediated cell–cell fusion and the formation of gp41 six-helix bundles, as does enfuvirtide.[10b] The bisindole derivative **2** also exhibits submicromolar inhibition of HIV-1 replication by interaction with the gp41 hydrophobic pocket in which compound **1** binds.[11] Small-molecule CD4 mimics with oxalamide and related substructures are another series of anti-HIV agents.[12] The representative BMS-448043 (**3**) exhibits subnanomolar anti-HIV activity by interaction with the CD4 binding pocket in gp120.[12d] These small-molecule entry inhibitors with potential oral bioavailability will provide alternative combination regimen(s) of anti-HIV agents for the treatment of drug-resistant variants.

In our efforts to develop novel anti-HIV compounds,[13] we have carried out the random screening of small molecules using multinuclear activation of a galactosidase indicator (MAGI) assay, in which the inhibitory activity of early-stage HIV infection, including virus attachment and membrane fusion to host cells, is evaluated. Among more than 30 000 compounds screened, 3,4-dihydro-2*H*,6*H*-pyrimido[1,2-*c*][1,3]benzothiazin-6-imine **4** (PD 404182) was identified as a potent anti-HIV agent lead (Fig. 1). Compound **4** was reported to be an enzyme inhibitor against 3-deoxy-D-manno-octulosonic acid 8-phosphate synthase[14] and phosphopantetheinyl transferase,[15] exerting

[a]*Graduate School of Pharmaceutical Sciences, Kyoto University, Sakyo-ku, Kyoto 606-8501, Japan. E-mail: soishi@pharm.kyoto-u.ac.jp, nfujii@pharm.kyoto-u.ac.jp; Fax: +81-75-753-4570; Tel: +81-75-753-4561*
[b]*Institute for Virus Research, Kyoto University, Sakyo-ku, Kyoto, 606-8507, Japan*

†Electronic supplementary information (ESI) available. See DOI: 10.1039/c2ob25904d

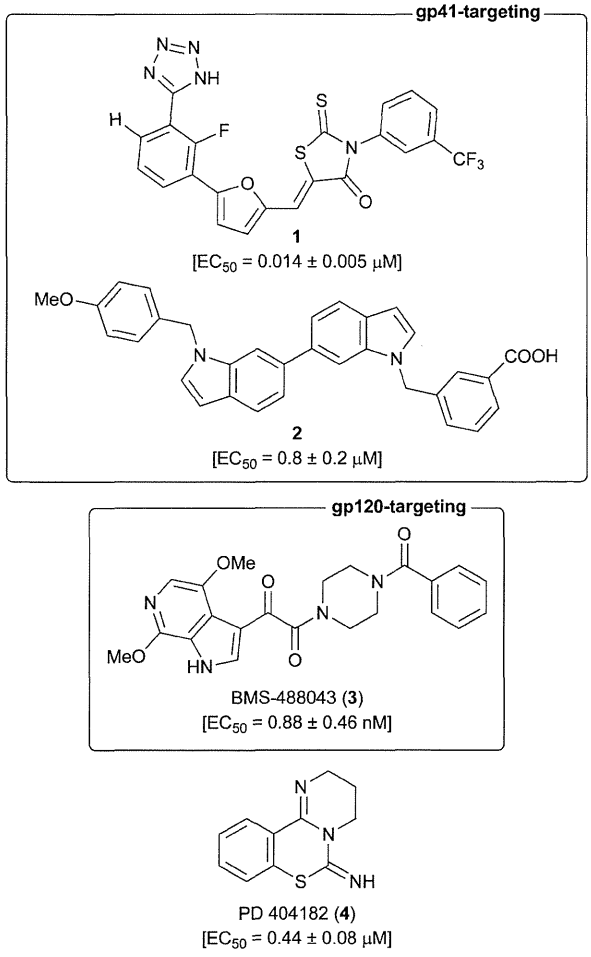

Fig. 1 Structures of newly reported anti-HIV compounds (**1**–**3**) targeting HIV-1 envelope proteins, and PD 404182 (**4**).

antimicrobial effects. In the course of our SAR investigations in this study, antiviral activities of **4** against HCV, HIV, and simian immunodeficiency virus were reported.[16,17] Although compound **4** exhibits virucidal effects at high concentrations, the mechanism of action and the target molecule remain ambiguous.[17]

Recently, we have established two independent approaches for the synthesis of PD 404182 derivatives (Scheme 1): C–H functionalization of 2-phenyl-1,4,5,6-tetrahydropyrimidine with water or *tert*-butylcarbamate in the presence of copper(II) acetate provides pyrimido[1,2-*c*][1,3]benzoxazine or pyrimido[1,2-*c*]-quinazoline in one or two step(s) (eqn (1), Scheme 1).[18] Alternatively, addition of 2-(2-halophenyl)-1,4,5,6-tetrahydropyrimidine to carbon disulfide, isocyanate, or isothiocyanate, and subsequent aromatic nucleophilic substitution (S_NAr) affords pyrimidobenzothiazines and -oxazines, and pyrimidoquinazolines (eqn (2), Scheme 1).[19] The derivatives obtained from these reactions were easily converted to the pyrimido[1,2-*c*][1,3]benzothiazin-6-imine scaffold. Our two synthetic methods provide a variety of PD 404182 derivatives from the corresponding benzaldehydes in a few steps and in good yields, facilitating the lead optimization process.[20] In this article, a SAR study of PD 404182 derivatives using these synthetic approaches is described.

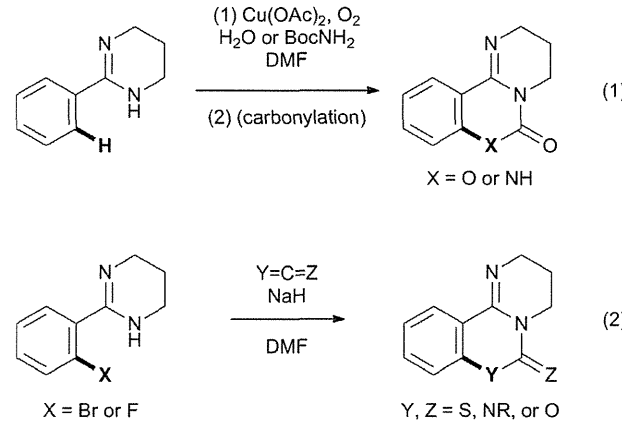

Scheme 1 Our synthetic methods for PD 404182 derivatives.

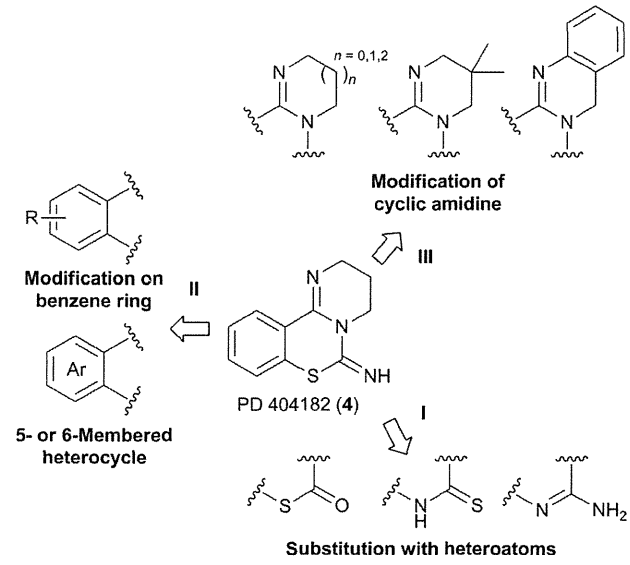

Fig. 2 Strategy for SAR study of PD 404182 (**4**).

Results and discussion

Strategy for the SAR study of PD 404182

PD 404182 consists of three components, namely a 1,3-thiazin-2-imine core, and left-fused benzene and cyclic amidine moieties (Fig. 2). In order to obtain detailed insights into the relationships between the compound structure and anti-HIV activity, we planned to investigate substituent effects on each component: (I) derivatives with various heteroatom (N, S, and O) arrangements on the 1,3-thiazin-2-imine core (Fig. 2); (II) pyrimido[1,2-*c*][1,3]-thiazin-6-imine derivatives fused with a substituted benzene ring or a five- or six-membered aromatic heterocycle; and (III) benzo-[*e*][1,3]thiazin-2-imine derivatives fused with a cyclic amidine ring with or without accessory alkyl or aryl groups.

Synthesis of pyrimido[1,2-*c*][1,3]benzothiazin-6-imines and related tricyclic heterocycles

Our investigation began with the synthesis of tricyclic heterocycles with different combinations of heteroatoms on the

1,3-thiazin-2-imine core. Previously, we reported syntheses of pyrimido[1,2-*c*][1,3]benzoxazine and pyrimido[1,2-*c*]quinazoline derivatives using copper(II)-mediated C–H functionalization;[18] this facilitates the introduction of oxygen or nitrogen functional groups at the *ortho*-position of 2-phenyl-1,4,5,6-tetrahydropyrimidine (**5**). Using compound **5** as a key starting material, a divergent approach was used for the preparation of a series of scaffolds (Scheme 2).

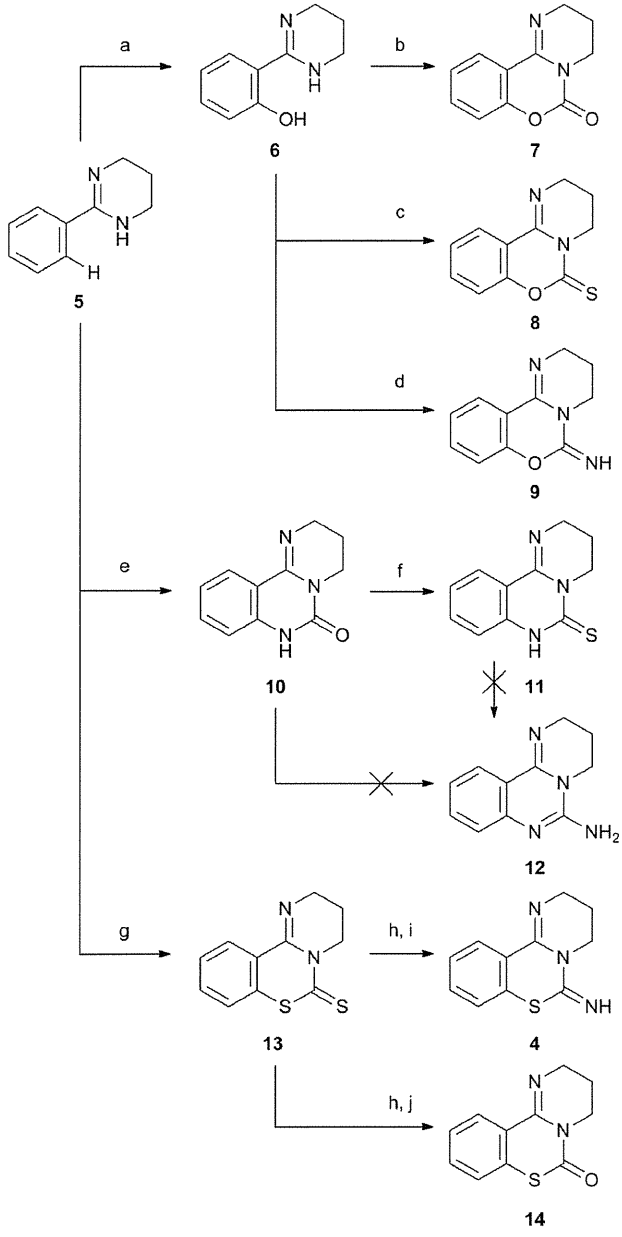

Scheme 2 Synthesis of PD 404182 derivatives with different combinations of heteroatoms. Reagents and conditions: (a) $Cu(OAc)_2$, H_2O, O_2, DMF, 130 °C, 69%; (b) triphosgene, TMEDA, CH_2Cl_2, 0 °C to rt, 70% [2 steps (a,b)]; (c) thiophosgene, Et_3N, CH_2Cl_2, 0 °C to rt, quant.; (d) BrCN, CH_2Cl_2, rt, 34%; (e) $Cu(OAc)_2$, $BocNH_2$, O_2, DMF, 130 °C, 53%; (f) Lawesson's reagent, xylene, reflux, 19%; (g) $Cu(OAc)_2$, CS_2, O_2, 1,4-dioxane, 130 °C, 11%; (h) NaOH, MeOH, H_2O, reflux; (i) BrCN, EtOH, reflux, 61% [2 steps (h,i)]; (j) triphosgene, Et_3N, CH_2Cl_2, 0 °C to rt, 65% [2 steps (h,j)].

A one-pot reaction for $Cu(OAc)_2$-mediated C–H functionalization of **5** and subsequent treatment with triphosgene provided a 1,3-oxazin-2-one derivative **7** (Scheme 2). The same one-pot procedure using thiophosgene produced a trace amount of the desired thiocarbonyl derivative **8**; treatment of the purified intermediate **6** with thiophosgene provided the desired 1,3-oxazine-2-thione **8** in high yield. 1,3-Oxazin-2-imine **9** was obtained by the reaction of **6** with BrCN.

The copper-mediated C–N bond formation of compound **5** with *tert*-butylcarbamate followed by spontaneous intramolecular cyclization afforded a pyrimido[1,2-*c*]quinazolin-6-one scaffold **10**, as demonstrated in our previous report (Scheme 2).[18] Subsequent treatment with Lawesson's reagent led to formation of the thiocarbonyl derivative **11**. Since no hydrolysis of the carbonyl or thiocarbonyl group of compound **10** or **11** for construction of the 2-aminoquinazoline structure in **12** occurred, an alternative approach starting from 2-aminobenzyl alcohol **15** was used for the synthesis of the 2-aminoquinazoline derivative **12** (Scheme 3). After protection and PCC oxidation of **15**, oxidative amidination[21] provided 2-(*p*-tosylamino)phenyltetrahydropyrimidine **17**. Deprotection followed by BrCN-mediated cyclization of **17** provided the expected 2-aminoquinazoline derivative **12**.

For the synthesis of pyrimido[1,2-*c*][1,3]benzothiazine derivatives, we adapted the C–H functionalization reaction for C–S bond formation (Scheme 2). After optimization of the reaction conditions, we found that exposure of compound **5** to CS_2 in the presence of $Cu(OAc)_2$ directly afforded a pyrimido[1,2-*c*][1,3]-benzothiazine-6-thione scaffold **13**. Hydrolysis of the thiocarbonyl group in **13** followed by treatment with BrCN or triphosgene provided 6-imino or 6-oxo derivatives (**4** or **14**), respectively.

Synthesis of pyrimido[1,2-*c*][1,3]thiazine derivatives with fused benzene and heterocycles

Pyrimido[1,2-*c*][1,3]thiazin-6-imine derivatives **28–30** with a series of fused ring systems were prepared by consecutive heterocumulene addition and S_NAr reactions (Scheme 4).[19] These reactions provide easy access to the construction of the 1,3-thiazin-2-imine derivatives and are more efficient than the diversity-oriented C–H functionalization approach. The oxidative amidination of aromatic aldehydes **18–20** with an accessory

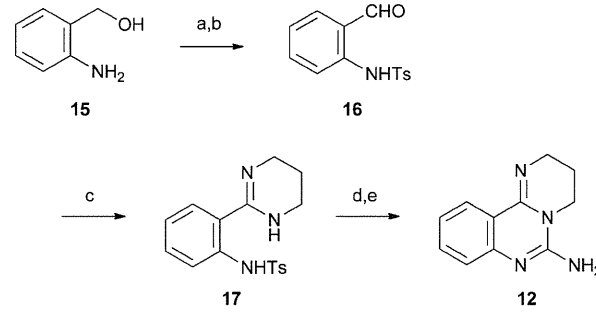

Scheme 3 Synthesis of 2-aminoquinazoline derivative **12**. Reagents and conditions: (a) *p*-TsCl, pyridine, $CHCl_3$, rt; (b) PCC, silica gel, CH_2Cl_2, rt, 80% [2 steps (a,b)]; (c) 1,3-propanediamine, I_2, K_2CO_3, *t*-BuOH, 70 °C, 98%; (d) conc. H_2SO_4, 100 °C, then NaOH, H_2O; (e) BrCN, EtOH, reflux, 66% [2 steps (d,e)].

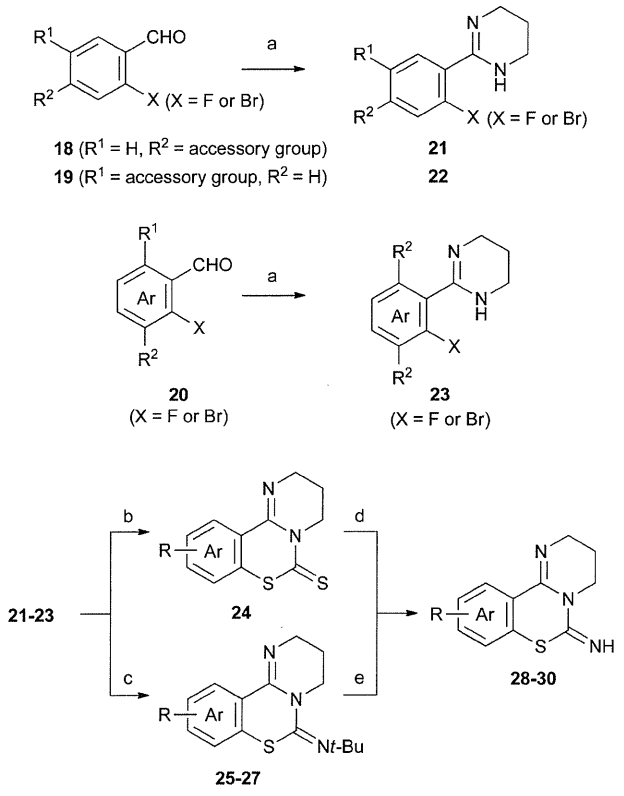

Scheme 4 Synthesis of pyrimido[1,2-*c*][1,3]thiazin-6-imine derivatives fused with substituted benzene and heterocycles (**28–30**). Reagents and conditions: (a) 1,3-propanediamine, I_2, K_2CO_3, *t*-BuOH, 70 °C, 58–91%; (b) NaH, CS_2, DMF, 80 °C, 67%-quant.; (c) NaH or *t*-BuOK, *t*-BuNCS, DMF or DMAc, −20–80 °C, 28–95%; (d) (i) NaOH, MeOH, H_2O, reflux, (ii) BrCN, EtOH, reflux, 32–68%; (e) TFA, MS4Å, $CHCl_3$, reflux, 63–92%.

functional group afforded the corresponding 2-phenyltetrahydropyrimidine derivatives **21–23**. The pyrimido[1,2-*c*][1,3]thiazine-6-thione scaffold **24** was obtained by additions of **21f,g,i** or **23s,t,u** to carbon disulfide followed by S_NAr-type C–S bond formation. The desired 6-imino derivatives **28f,g,i** and **30s,t,u** were obtained *via* hydrolysis of the thiocarbonyl group of **24** followed by BrCN treatment. Alternatively, reactions of other 2-phenyltetrahydropyrimidines **21–23** with *tert*-butyl isothiocyanate afforded *N*-(*t*-Bu)-protected thiazinimine derivatives **25–27**, which were treated with TFA to provide the expected products **28–30**.

The intermediates **25e**, **25k**, and **26k** were subjected to further manipulations to obtain the functionalized derivatives (Scheme 5). The nitro group of **25e** was reduced by hydrogenation to form the 9-amino derivative **31**. Alkylation of **31** afforded the 9-(*N*-methylamino) derivative **25b** (eqn (1), Scheme 5). The 9-acetamide derivative **25c** was obtained by treatment of **31** with acetic anhydride (eqn (2), Scheme 5). Sandmeyer reaction of **31** gave the 9-azide derivative **25p** (eqn (3), Scheme 5). Me_2N- and MeO-substituted derivatives (**25a**, **26a**, and **26f**) were obtained by Me_2NH-mediated *N*-arylation[22] of the 9-bromo **25k** and 10-bromo derivatives **26k**, and NaOMe-mediated Ullmann coupling[23] of **26k**, respectively (eqn (4) and

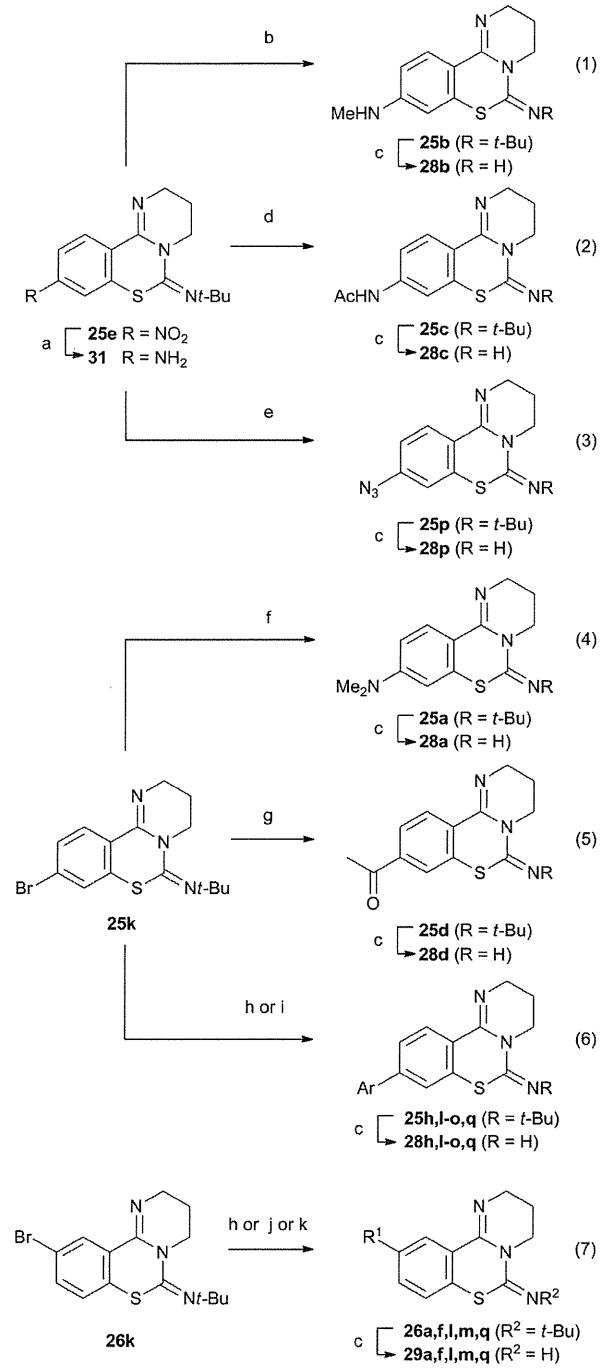

Scheme 5 Synthesis of 9- or 10-substituted pyrimido[1,2-*c*][1,3]benzothiazin-6-imine derivatives. Reagents and conditions: (a) H_2, Pd/C, EtOH, rt, 88%; (b) NaOMe, $(CH_2O)_n$, MeOH, reflux, then $NaBH_4$, 91%; (c) TFA, MS4Å, $CHCl_3$, reflux, 37–95%; (d) Ac_2O, DMAP, Et_3N, CH_2Cl_2, rt, quant.; (e) $NaNO_2$, AcOH, H_2O, 0 °C, then NaN_3, 70%; (f) $Pd(OAc)_2$, *t*-Bu_3P, $NHMe_2$, THF, KO*t*-Bu, toluene, reflux, quant.; (g) 2-hydroxyethylvinylether, $Pd(OAc)_2$, 1,3-bis(diphenylphosphino)-propane, K_2CO_3, H_2O, 90 °C, 13% [2 steps (g,c)]; (h) R-$B(OH)_2$ or R-Bpin, $Pd(PPh_3)_4$, $PdCl_2(dppf)\cdot CH_2Cl_2$, K_2CO_3, toluene or 1,4-dioxane, EtOH, H_2O, reflux, 62–96%; (i) *n*-$BuB(OH)_2$, $Pd_2(dba)_3$, P(*t*-Bu)$_3$, $CsCO_3$, 1,4-dioxane, reflux, 6% (for **25h**); (j) $Pd(Pt\text{-}Bu)_2$, $NHMe_2$, THF, KO*t*-Bu, toluene, 170 °C, 67% (for **26a**); (k) CuBr, NaOMe, MeOH, DMF, reflux, 40% (for **26f**).

(7), Scheme 5). The 9-acetyl derivative **25d** was obtained by Heck reaction[24] of **25k** with 2-hydroxyethyl vinyl ether (eqn (5), Scheme 5). Other derivatives with a variety of functional groups (**25h,l–o,q** and **26l,m,q**) were synthesized by Suzuki–Miyaura coupling reactions[25] of **25k** and **26k** with boronic acids or their pinacol esters (eqn (6) and (7), Scheme 5). Final deprotection of the *tert*-butyl group in **25** and **26** afforded the 9- or 10-substituted pyrimido[1,2-*c*][1,3]benzothiazine derivatives **28** and **29**, respectively.

Synthesis of benzo[*e*][1,3]thiazine derivatives with fused cyclic amidines

Benzo[*e*][1,3]thiazine derivatives with various ring-sized and/or modified cyclic amidine moieties **35** were also synthesized by the consecutive heterocumulene addition and S_NAr reactions (Scheme 6). Oxidative amidination using several diamines **32** proceeded efficiently to form five- or six-membered rings (**33a–d**). The same reaction for the seven-membered amidine (**33e**) was incomplete, but purification of the Boc-protected amidine **36** followed by subsequent deprotection of the Boc group gave the pure seven-membered amidine **33e**. The resulting amidines were converted to cyclic-amidine-fused benzo[*e*][1,3]-thiazin-2-imines **34** *via tert*-butyl isothiocyanate addition and an S_NAr reaction. TFA-mediated deprotection gave the expected derivatives **35**.

Structure–activity relationships of the central heterocyclic core in pyrimido[1,2-*c*][1,3]benzothiazines

Initially, the structural requirements of the 1,3-thiazin-2-imine core substructure in **4** (PD 404182) for anti-HIV activity were investigated (Table 1). The antiviral activities against the HIV-1_{IIIB} strain were evaluated using the MAGI assay. Substitution of the imino group in **4** with a carbonyl group (**14**) resulted in a significant decrease in anti-HIV activity (EC_{50} = 8.94 μM). Pyrimido[1,2-*c*][1,3]benzoxazines (**7–9**), pyrimido [1,2-*c*]quinazolines (**10–12**), and pyrimido[1,2-*c*][1,3]benzothiazine-6-thione (**13**), in which the 1-sulfur and/or 2-imino groups in **4** were modified, showed no activity. These results suggested that both the 1-sulfur atom and the 2-imino group are indispensable functional groups for the inhibitory activity against HIV infection, and may be involved in potential interactions with the target molecules.

Structure–activity relationships of the benzene substructure in pyrimido[1,2-*c*][1,3]benzothiazine

A series of derivatives with modification of the benzene substructure in the pyrimido[1,2-*c*][1,3]benzothiazine were evaluated for anti-HIV activity (Table 2). The addition of positively charged *N*,*N*-dimethylamino (**28a**) and *N*-methylamino groups (**28b**) at the 9-position significantly decreased the anti-HIV activity. The 9-acetamide group (**28c**), which has hydrogen-bond donor/acceptor abilities, also attenuated the bioactivity. The acetyl (**28d**) and nitro (**28e**) groups, with hydrogen acceptor properties, induced slight decreases in the anti-HIV activity. In contrast, derivatives with less-polarized substituents (**28f–o** and

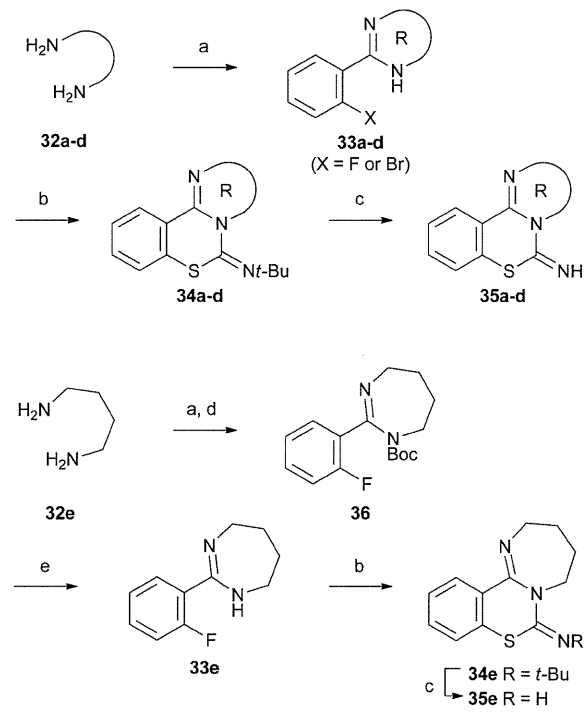

Scheme 6 Synthesis of benzo[*e*][1,3]thiazine derivatives with fused cyclic amidines. Reagents and conditions: (a) 2-fluorobenzaldehyde or 2-bromobenzaldehyde, I_2, K_2CO_3, *t*-BuOH, 70 °C, 68–79%; (b) NaH, *t*-BuNCS, DMF, rt −80 °C, 18–50%; (c) TFA, MS4Å, $CHCl_3$, reflux, 16–86%; (d) Boc_2O, Et_3N, DMAP, CH_2Cl_2, rt, 37% [2 steps (a,d)]; (e) TFA, CH_2Cl_2, reflux, 80%.

Table 1 SARs for 1,3-thiazin-2-imine core

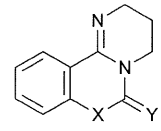

Compound	X	Y	EC_{50} (μM)[a]
4	S	NH	0.44 ± 0.08
7	O	O	>10
8	O	S	>10
9	O	NH	>10
10	NH	O	>10
11	NH	S	>10
12	NH	NH	>10
13	S	S	>10
14	S	O	8.94 ± 1.07

[a] EC_{50} values were the concentration that blocks HIV-1 infection by 50% and derived from three independent experiments.

28q) at this position generally reproduced the potent anti-HIV activity of **4**. In terms of the electron-donating or -withdrawing properties of the substituent groups on the benzene substructure, good correlations were not observed. For example, the electron-donating methoxy (**28f**), methyl (**28g**), and *n*-butyl groups (**28h**), and the electron-withdrawing fluoro (**28i**) and trifluoromethyl groups (**28j**) exhibited similar anti-HIV activities (EC_{50} =

Table 2 SARs for benzene part

Compound		EC_{50} (μM)[a]	Compound		EC_{50} (μM)[a]
	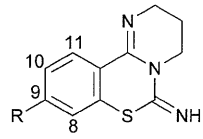		**30r**	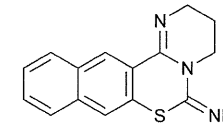	0.56 ± 0.13
4	R = H	0.44 ± 0.08			
28a	R = NMe_2	4.74 ± 1.07			
28b	R = NHMe	>10			
28c	R = NHAc	>10	**30s**	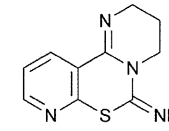	2.55 ± 0.26
28d	R = COMe	1.44 ± 0.33			
28e	R = NO_2	1.13 ± 0.18			
28f	R = OMe	0.57 ± 0.09			
28g	R = Me	0.49 ± 0.10			
28h	R = *n*-butyl	0.44 ± 0.09			
28i	R = F	0.50 ± 0.07	**30k**	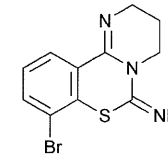	>10
28j	R = CF_3	0.53 ± 0.12			
28k	R = Br	0.25 ± 0.09			
28l	R = Ph	0.24 ± 0.04			
28m	R = vinyl	0.18 ± 0.05			
28n	R = styryl	0.25 ± 0.05			
28o	R = pentenyl	0.24 ± 0.11	**30t**	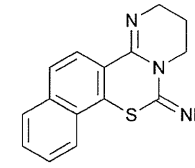	>10
28p	R = N_3	0.43 ± 0.06			
28q	R = C_6H_4(4-Bz)	0.53 ± 0.12			
	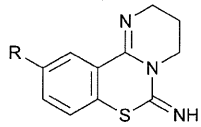		**30i**	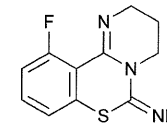	1.68 ± 0.19
29a	R = NMe_2	2.12 ± 0.26			
29e	R = NO_2	3.00 ± 0.59			
29f	R = OMe	0.53 ± 0.04			
29g	R = Me	0.38 ± 0.04			
29k	R = Br	0.24 ± 0.05			
29l	R = Ph	0.24 ± 0.05	**30u**	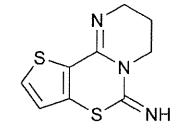	>10
29m	R = vinyl	0.40 ± 0.09			
29q	R = C_6H_4(4-Bz)	0.67 ± 0.16			

[a] EC_{50} values were the concentration that blocks HIV-1 infection by 50% and derived from three independent experiments.

0.44–0.57 μM), indicating that the antiviral activity is independent of the electronic state of the 1,3-benzothiazin-2-imine core in forming potential π-stacking interaction(s) with the target molecules. Among the hydrophobic substituents at this position, bromo (**28k**), phenyl (**28l**), vinyl (**28m**), styryl (**28n**), and pentenyl groups (**28o**) induced inhibitory activity two or three times greater than that of **4** (EC_{50} = 0.18–0.25 μM). Modification with photoreactive azido (**28p**) and benzoylphenyl groups (**28q**) maintained the inhibitory activity; these could be used as probe molecules to identify the target molecule(s) of **4**.[26]

Similar SARs were observed for modification at the 10-position of pyrimido[1,2-*c*][1,3]benzothiazine. Addition of positively charged *N*,*N*-dimethylamino (**29a**) and polarized nitro groups (**29e**) reduced the anti-HIV activity (EC_{50} = 2.12 and 3.00 μM, respectively). Hydrophobic groups including methoxy (**29f**), methyl (**29g**), bromo (**29k**), phenyl (**29l**), vinyl (**29m**), and 4-benzoylphenyl (**29q**) (EC_{50} = 0.24–0.67 μM) had favorable effects on the bioactivity, suggesting potential hydrophobic interactions of these additional functional groups with the target molecule(s).

Further miscellaneous modifications of benzothiazine substructure were also investigated (Table 2). The naphtho[2,3-*e*][1,3]thiazine derivative **30r**, with a 9,10-fused benzene, exhibited anti-HIV activity equipotent to that of the parent **4** (EC_{50} = 0.56 μM). A 6-fold decrease in the anti-HIV activity of the pyridine-fused pyrido[3,2-*e*][1,3]thiazine derivative (**30s**) was observed (EC_{50} = 2.55 μM). In addition, introduction of 8-bromo (**30k**) and 8,9-fused benzene (**30t**, naphtho[2,1-*e*][1,3]thiazine) substituents on benzothiazine resulted in a loss of activity, suggesting that modification at the 8-position was inappropriate for favorable interactions with the target molecule(s). The 11-fluoro derivative **30i** and thiophene-fused **30u**, which has a 5-6-6 framework (thieno[2,3-*e*][1,3]thiazine), exhibited four times lower and no inhibitory potencies, respectively.

Structure–activity relationships of cyclic amidine part of pyrimido[1,2-*c*][1,3]benzothiazine

A SAR study of the top-right cyclic amidine substructure was carried out. The five-membered dihydroimidazole derivative **35a** had no anti-HIV activity (Table 3), suggesting that the five-membered ring may impair the critical interactions with the target molecule(s) *via* its small-sized ring strain or indirect effects on the thiazinimine core with a possibly altered conformation. Similarly, compound **35b** with the phenyl-fused dihydropyrimidine substructure showed lower inhibitory activity (EC_{50} = 3.78 μM). Appending one or two methyl groups on the six-membered pyrimidine (**35c** and **35d**) induced 1.5- to 2-fold higher inhibitory potencies (EC_{50} = 0.35 and 0.24 μM, respectively) compared with that of the parent compound **4**. In addition, compound **35e** with a seven-membered tetrahydro-1,3-diazepine substructure exhibited similar anti-HIV activity to that of **4** (EC_{50} = 0.31 μM).

Mechanistic studies of anti-HIV pyrimido[1,2-*c*][1,3]-benzothiazin-6-imines and related tricyclic heterocycles

To investigate the mechanism of action of PD 404182 derivatives, a time of drug addition study was carried out (Fig. 3). In this experiment, the anti-HIV activity profiles of **4**[27] and its derivatives **29k**[27] were compared with those of well-known anti-HIV agents such as an adsorption inhibitor (DS 5000),[28] fusion inhibitor [enfuvirtide (T-20)],[5] NRTI (AZT),[29] NNRTI (nevirapine),[30] and integrase inhibitor (raltegravir).[6] After inoculation of HeLa-CD4/CCR5-LTR/β-gal cells with HIV-1_{IIIB}, each anti-HIV-1 drug was added at a 90% inhibitory effect concentration at the indicated time points. The inhibitory effects on the infection were determined by counting the blue cells 48 h later. This investigation revealed that compound **4** (PD 404182) had an inhibitory profile in the early stage of viral infection similar to those of DS 5000 and enfuvirtide (Fig. 3). Identical profiles were observed for derivative **29k**.

Table 3 SARs for cyclic amidine

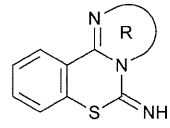

Compound		EC_{50} (μM)[a]
4	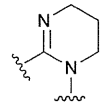	0.44 ± 0.08
35a		>10
35b	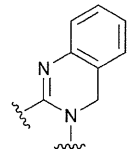	3.78 ± 1.39
35c	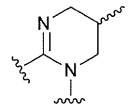	0.35 ± 0.09
35d	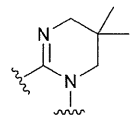	0.24 ± 0.04
35e	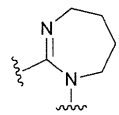	0.31 ± 0.06

[a] EC_{50} values were the concentration that blocks HIV-1 infection by 50% and derived from three independent experiments.

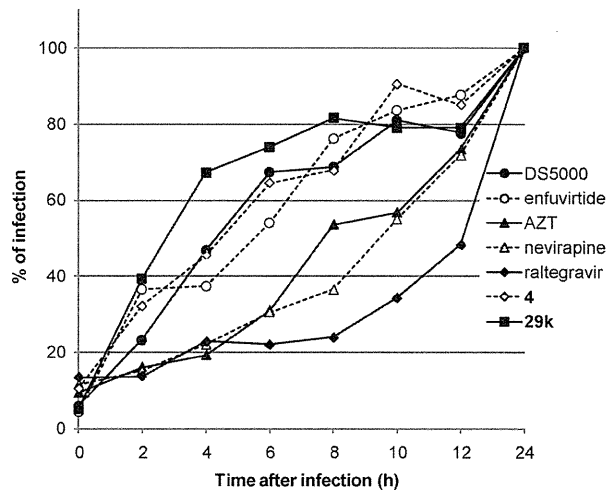

Fig. 3 Time of drug addition profiles for infection by HIV-1_{IIIB} strain of HeLa-CD4/CCR5-LTR/β-gal cells.

Table 4 Anti-HIV activity of **4** and **35d** against other HIV strains

Strain	EC_{50} (μM)[a]	
	4	**35d**
HIV-1_{NL4-3}	0.38 ± 0.06	0.25 ± 0.03
HIV-1_{BaL}	0.37 ± 0.06	0.16 ± 0.02
HIV-2_{EHO}	0.31 ±0.06	0.17 ± 0.03
HIV-2_{ROD}	0.30 ± 0.06	0.11 ± 0.03

[a] EC_{50} values were the concentration that blocks HIV infection by 50% and derived from three independent experiments.

To gain additional insights into the mechanism of action of PD 404182 derivatives, the antiviral activities against other HIV subtypes were evaluated (Table 4). Compound **4** was effective against not only HIV-1_{IIIB} but also other two HIV-1 strains (HIV-1_{NL4-3} and HIV-1_{BaL}) with similar potency. Both HIV-1_{IIIB} and HIV-1_{NL4-3} strains utilize CXCR4 as a coreceptor for entry, while HIV-1_{BaL} strain does CCR5, indicating that chemokine receptors CXCR4 and CCR5 are not the molecular targets of PD 404182 derivatives. The similar level of antiviral activity of **4** against HIV-2 (HIV-2_{EHO} and HIV-2_{ROD}), which is mainly distributed in West Africa, was observed. Highly potent inhibitory activities of a derivative **35d**[27] against these HIV strains were observed, as in the case of the SAR study of the HIV-1_{IIIB} strain discussed above. It has been well known that NNRTIs are not effective against HIV-2, highlighting that PD 404182 derivatives do not act as NNRTIs. Although PD 404182 derivatives and enfuvirtide showed similar anti-HIV-1 profile in the time of drug addition assay, HIV-2_{EHO} and HIV-2_{ROD} infection were affected by PD 404182 derivatives, in contrast with the less effective enfuvirtide,[31] suggesting that PD 404182 derivatives may not be directed at the HIV gp41 envelope protein. Recent reports have suggested that the antiviral activities of compound **4** against HIV, HCV, and pseudotype lentiviruses were derived from disruption of the structural integrities of virions.[17] Although the mechanism of action of PD 404182 derivatives is not fully understood at this stage, the unidentified biomolecule(s) in viruses or host cells, including envelope protein(s), lipid membranes and/or sugar chain(s), could be promising molecular targets for this new class of anti-HIV agents.

Conclusion

In conclusion, we have designed and synthesized PD 404182 derivatives for a novel series of anti-HIV agents. Comprehensive SAR studies demonstrated that the 6-6-6 fused pyrimido[1,2-*c*]-[1,3]benzothiazine scaffold and the heteroatom arrangement in the thiazinimine moiety are indispensable for the inhibitory activity of **4** (PD 404182) against HIV infection. Optimization studies of the benzene and cyclic amidine rings indicate that the introduction of a hydrophobic group on the benzene ring and the amidine group is more effective in improving the antiviral activity, giving potential favorable interaction(s) with the target molecule(s). In addition, PD 404182 derivatives could be promising agents for treatment of HIV-2 infection. We also revealed, using time of drug addition experiments, that PD 404182 derivatives prevent the HIV infection process at an early stage. For iterative molecular design of more effective derivatives based on binding modes, the identification of the target molecule(s) of PD 404182 derivatives is being investigated using derivatives such as **28p** and **28q**.

Experimental section

General

^{1}H NMR spectra were recorded using a JEOL AL-400 or a JEOL ECA-500 spectrometer. Chemical shifts are reported in δ (ppm) relative to Me_4Si as an internal standard. ^{13}C NMR spectra were referenced to the residual solvent signal. Exact mass (HRMS) spectra were recorded on a JMS-HX/HX 110A mass spectrometer. Melting points were measured by a hot stage melting point apparatus (uncorrected). For flash chromatography, Wakogel C-300E (Wako) or aluminium oxide 90 standardized (Merck) were employed. For preparative TLC, TLC Silica gel 60 F_{254} (Merck), TLC Aluminium oxide 60 F_{254} basic (Merck), or NH_2 Silica Gel 60 F_{254} Plate (Wako) were employed. For analytical HPLC, a Cosmosil 5C18-ARII column (4.6 × 250 mm, Nacalai Tesque, Inc., Kyoto, Japan) was employed with method A [a linear gradient of CH_3CN containing 0.1% (v/v) TFA] or method B [a linear gradient of CH_3CN containing 0.1% (v/v) NH_3] at a flow rate of 1 cm^3 min^{-1} on a Shimadzu LC-10ADvp (Shimadzu Corp., Ltd., Kyoto, Japan), and eluting products were detected by UV at 254 nm. The purity of the compounds was determined by combustion analysis or HPLC analysis as >95% unless otherwise stated.

General procedure of oxidative amidination: synthesis of 2-(3-bromo-2-fluorophenyl)-1,4,5,6-tetrahydropyrimidine (23k). To a solution of 3-bromo-2-fluorobenzaldehyde **20k** (0.71 g, 3.5 mmol) in *t*-BuOH (33 cm^3) was added propylenediamine (285.4 mg, 3.9 mmol). The mixture was stirred at 70 °C for 30 min, and then K_2CO_3 (1.45 g, 10.5 mmol) and I_2 (1.11 g, 4.4 mmol) were added. After being stirred at the same temperature for 3 h, the mixture was quenched with sat. Na_2SO_3. The organic layer was separated and concentrated. The resulting solid was dissolved in H_2O, and then pH was adjusted to 12–14 with 2N NaOH. The whole was extracted with $CHCl_3$. The extract was dried over $MgSO_4$. After concentration, the resulting solid was recrystallized from $CHCl_3$–*n*-hexane to give compound **23k** as colorless crystals (0.62 g, 69%): mp 99 °C; IR (neat) ν_{max}/cm^{-1}: 1624 (C=N); δ_H (400 MHz; $CDCl_3$; Me_4Si) 1.84–1.89 (2H, m, CH_2), 3.50 (4H, t, J = 5.7 Hz, 2 × CH_2), 5.13 (1H, br s, NH), 7.03 (1H, td, J = 8.0, 0.9 Hz, Ar), 7.54 (1H, ddd, J = 8.0, 6.4, 1.3 Hz, Ar) and 7.69 (1H, ddd, J = 8.0, 6.5, 1.3 Hz, Ar). δ_C (100 MHz; $CDCl_3$) 20.6, 42.1 (2C), 109.6 (d, J = 22.3 Hz), 125.1 (d, J = 4.1 Hz), 126.3 (d, J = 13.2 Hz), 129.8 (d, J = 3.3 Hz), 134.3, 150.8 and 156.3 (d, J = 248.3 Hz); δ_F (500 MHz; $CDCl_3$) −110.7; *Anal.* Calc. for $C_{10}H_{10}BrFN_2$: C, 46.72; H, 3.92; N, 10.90. Found: C, 46.64; H, 4.10; N, 10.93%.

General procedure of CS_2-mediated cyclization for pyrimido-[1,2-*c*][1,3]benzothiazine-6-thiones 24: synthesis of 3,4-dihydro-2*H*,6*H*-pyrimido[1,2-*c*]thieno[2,3-*e*][1,3]thiazin-6-thione (24u). To a mixture of 2-(3-bromothiophen-2-yl)-1,4,5,6-tetrahydropyrimidine **23u** (122.6 mg, 0.50 mmol) and NaH (40.0 mg,